Aloe-emodin ameliorates chronic kidney disease fibrosis by inhibiting PI3K-mediated signaling pathway

Ming Chen,[1,2]* Wenhui Zhu,[3]* Yao Chen,[4]* Jingying Shang,[1] Wenfan Wang,[3] Xiaoming Yan,[2] Peng Liu,[4] Yabin Zhou[5]

[1]Heilongjiang university of Chinese Medicine, Harbin
[2]Renal Division, Department of Medicine, Heilongjiang Academy of Chinese Medicine Sciences, Harbin
[3]College of Traditional Chinese Medicine, Changchun University of Chinese Medicine, Changchun
[4]Department of Nephrology, Xiyuan Hospital of China Academy of Chinese Medical Sciences, Beijing
[5]The First Affiliated Hospital of Heilongjiang University of Chinese Medicine, Harbin, China

*These authors contributed equally to this work.

ABSTRACT

Chronic kidney disease (CKD) impacts a vast number of individuals worldwide, culminating in renal fibrosis. Renal fibrosis serves as the main reason for end-stage renal failure. However, the current targeted treatment methods for renal fibrosis remain scarce. Aloe-emodin (AE) is a naturally occurring compound discovered in rhubarb and aloe. In this research, we investigated the underlying mechanisms of AE in adenine-induced mouse renal fibrosis models and TGFβ-1 stimulated renal tubular epithelial cells (HK-2). It was discovered that AE not only decelerated the decline of renal function in adenine-treated mice but also suppressed the expression of Collagen I and Fibronectin. Furthermore, network pharmacology analysis suggested that AE's treatment of renal fibrosis might function *via* the PI3K/Akt/GSK3β signaling pathway. *In vivo* and *in vitro* Western blot and immunofluorescence findings demonstrate that AE significantly resists the advancement of renal fibrosis by inhibiting α-smooth muscle actin and vimentin. Simultaneously, findings from 740Y-P (a PI3K agonist) and siRNA (PI3K) indicate that AE inhibits the expression of the PI3K/Akt/GSK3β cascade by lowering PI3K's phosphorylation level. From a mechanistic perspective, through molecular docking and plasmid transfection, the specific base sequence of PI3K in HK-2 cells was altered for experimental validation. The outcomes illustrate that AE can directly bind with PI3K, inhibiting its activation, impeding the PI3K/Akt/GSK3β signal transmission, thereby ultimately suppressing renal fibrosis progression. In conclusion, PI3K/Akt/GSK3β is a potential therapeutic target for CKD-related renal fibrosis, making AE a promising new treatment alternative for this condition.

Key words: renal fibrosis; network pharmacology; PI3K/Akt/GSK3β signaling pathway.

Correspondence: Yabin Zhou, The First Affiliated Hospital of Heilongjiang University of Chinese Medicine, No. 24, Heping Street, Harbin, 150036, China. E-mail: zhouyabinhljzyydx@126.com

Contributions: MC, WZ, PL, YZ, conceived and designed the experiments; WZ, YC, MC, experiments performing, manuscript drafting; WW, XY, experiments guidance; PL, funding acquisition. All the authors read and approved the final version of the manuscript and agreed to be accountable for all aspects of the work. Xiaoming Yan (yanxiaoming604@126.com) and Peng Liu (drliupeng@sina.cn) should be considered as co-corresponding authors .

Conflict of interests: the authors declare no conflicts of interest.

Ethics approval: all animal experiments in this study were conducted in accordance with the protocols approved by the Ethics Committee for Laboratory Animal Welfare of China-Japan Friendship Hospital (Approval No. zryhyy21-22-01-01). The date of approval is 3 January 2022.

Funding: this work was supported by the National Natural Science Foundation of China (No. 82274489), the Beijing Natural Science Foundation of China (No. 7232326) and the Heilongjiang Provincial Natural Science Foundation of China (No. LH2021H070).

Availability of data and materials: the data supporting the findings of this study are available from the corresponding author upon reasonable request.

Aloe-emodin ameliorates chronic kidney disease fibrosis by inhibiting PI3K-mediated signaling pathway

Ming Chen,[1,2]* Wenhui Zhu,[3]* Yao Chen,[4]* Jingying Shang,[1] Wenfan Wang,[3] Xiaoming Yan,[2] Peng Liu,[4] Yabin Zhou[5]

[1]Heilongjiang university of Chinese Medicine, Harbin
[2]Renal Division, Department of Medicine, Heilongjiang Academy of Chinese Medicine Sciences, Harbin
[3]College of Traditional Chinese Medicine, Changchun University of Chinese Medicine, Changchun
[4]Department of Nephrology, Xiyuan Hospital of China Academy of Chinese Medical Sciences, Beijing
[5]The First Affiliated Hospital of Heilongjiang University of Chinese Medicine, Harbin, China

*These authors contributed equally to this work.

ABSTRACT

Chronic kidney disease (CKD) impacts a vast number of individuals worldwide, culminating in renal fibrosis. Renal fibrosis serves as the main reason for end-stage renal failure. However, the current targeted treatment methods for renal fibrosis remain scarce. Aloe-emodin (AE) is a naturally occurring compound discovered in rhubarb and aloe. In this research, we investigated the underlying mechanisms of AE in adenine-induced mouse renal fibrosis models and TGFβ-1 stimulated renal tubular epithelial cells (HK-2). It was discovered that AE not only decelerated the decline of renal function in adenine-treated mice but also suppressed the expression of Collagen I and Fibronectin. Furthermore, network pharmacology analysis suggested that AE's treatment of renal fibrosis might function *via* the PI3K/Akt/GSK3β signaling pathway. *In vivo* and *in vitro* Western blot and immunofluorescence findings demonstrate that AE significantly resists the advancement of renal fibrosis by inhibiting α-smooth muscle actin and vimentin. Simultaneously, findings from 740Y-P (a PI3K agonist) and siRNA (PI3K) indicate that AE inhibits the expression of the PI3K/Akt/GSK3β cascade by lowering PI3K's phosphorylation level. From a mechanistic perspective, through molecular docking and plasmid transfection, the specific base sequence of PI3K in HK-2 cells was altered for experimental validation. The outcomes illustrate that AE can directly bind with PI3K, inhibiting its activation, impeding the PI3K/Akt/GSK3β signal transmission, thereby ultimately suppressing renal fibrosis progression. In conclusion, PI3K/Akt/GSK3β is a potential therapeutic target for CKD-related renal fibrosis, making AE a promising new treatment alternative for this condition.

Key words: renal fibrosis; network pharmacology; PI3K/Akt/GSK3β signaling pathway.

Correspondence: Yabin Zhou, The First Affiliated Hospital of Heilongjiang University of Chinese Medicine, No. 24, Heping Street, Harbin, 150036, China. E-mail: zhouyabinhljzyydx@126.com

Contributions: MC, WZ, PL, YZ, conceived and designed the experiments; WZ, YC, MC, experiments performing, manuscript drafting; WW, XY, experiments guidance; PL, funding acquisition. All the authors read and approved the final version of the manuscript and agreed to be accountable for all aspects of the work. Xiaoming Yan (yanxiaoming604@126.com) and Peng Liu (drliupeng@sina.cn) should be considered as co-corresponding authors .

Conflict of interests: the authors declare no conflicts of interest.

Ethics approval: all animal experiments in this study were conducted in accordance with the protocols approved by the Ethics Committee for Laboratory Animal Welfare of China-Japan Friendship Hospital (Approval No. zryhyy21-22-01-01). The date of approval is 3 January 2022.

Funding: this work was supported by the National Natural Science Foundation of China (No. 82274489), the Beijing Natural Science Foundation of China (No. 7232326) and the Heilongjiang Provincial Natural Science Foundation of China (No. LH2021H070).

Availability of data and materials: the data supporting the findings of this study are available from the corresponding author upon reasonable request.

Introduction

Chronic kidney disease (CKD) impacts approximately 10% of people worldwide, presenting a growing health concern. The defining characteristic of this condition is the irreversible deterioration of kidney function over time, which ultimately progresses to uremia.[1] Kidney fibrosis is a common consequence of progressive renal diseases.[2] The process involves extracellular matrix (ECM) deposition, cellular scarring, and kidney structure destruction, eventually leading to end-stage kidney disease.[3] Although there has been further understanding of the pathophysiology of CKD in recent years, current treatment strategies are still limited to slowing the disease's progression rather than reversing established kidney fibrosis.[4] Chinese Herbal Medicine (CHM), after decades of extensive research, has shown that some medicinal herbs, especially their extracted compounds, can treat various diseases and gradually elucidate their potential mechanisms.[5,6] Therefore, CHM may offer a novel and effective solution for managing CKD fibrosis.[7]

Aloe-emodin (AE) is an isomer of emodin, an anthraquinone derivative commonly found in aloe and rhubarb. It has garnered attention due to its wide range of biological activities, including immunomodulatory, anti-viral, anti-inflammatory, neuroprotective, anti-cancer and hepatoprotective properties.[8] It shows remarkable potential in treating various diseases such as inflammatory diseases, growth disorders, sepsis, malaria, liver fibrosis, flu, type 2 diabetes and psoriasis.[9] Notably, AE can inhibit the proliferation of transformed rat hepatic stellate cells by activating Caspase-9 in the mitochondrial pathway to induce apoptosis;[10] it can also significantly suppress the production of type I collagen and the expression α-smooth muscle actin (α-SMA) in hepatic stellate cells.[11,12] Current research has revealed AE's capability to combat fibrosis, offering new insights into therapeutic approaches for kidney fibrosis. Multiple mechanisms of kidney fibrosis have been confirmed. These include the TGF-β/Smad,[13] PI3K/Akt[14], Wnt/β-Catenin,[15] MAPK/ERK,[16] and JAK/STAT[17]signaling pathways. Among them, the PI3K/Akt signaling pathway is one of the key intracellular signaling pathways that modulate a variety of cellular processes such as proliferation, survival, growth, and metabolism.[18] This pathway has a strong impact on the pathophysiological process of excessive deposition of ECM proteins[19] - one of the hallmark features of fibrotic kidney disease. Liu *et al.* discovered that the Bupi Yishen formula inhibits the activity of PI3K/AKT signaling induced by adenine in rat kidneys and reduces the activation of PI3K/AKT signaling in TGF-β1-induced human proximal renal tubular cells (HK-2) in a dose-dependent manner, thereby alleviating kidney fibrosis.[20] Meanwhile, Glycogen synthase kinase 3 beta (GSK3β) is an important downstream target in the PI3K/Akt signaling pathway and participates in various biological mechanisms.[21] Research has found that inhibiting GSK3β can reduce fibrosis in AKI mice.[22] The results of these studies indicate that GSK3β plays a role in the pathogenesis of renal fibrosis following injury. Furthermore, inhibition of GSK3β prevented the progression of fibrosis even after injury had occurred, highlighting its importance as a therapeutic target. Based on the above analysis, we can hypothesize that modulating the activity of the PI3K/Akt/GSK3β signaling axis can help control or reverse the progression of kidney fibrosis caused by other chronic kidney diseases. Therefore, our study proposed to delve into the protective effects of AE on CKD-induced renal fibrosis, focusing on its effects on the PI3K/Akt/GSK-3β signaling axis. We used adenine-induced C57BL/6 mice and TGF-β1-induced HK-2 cells to investigate the effects of AE on CKD fibrosis. Additionally, we investigated the molecular mechanisms of AE in CKD fibrosis and the role of the PI3K/Akt/GSK3β signaling pathway using network pharmacology. This study aims to verify that AE improves renal fibrosis by inhibiting the PI3K/Akt/GSK3β pathway.

Materials and Methods

Prediction of targets

The targets of AE were acquired from the Traditional Chinese Medicine System Pharmacology Database (TCMSP, https://old.tcmsp-e.com/tcmsp.php). The protein name was also normalized through the UniProtKB database (http://www.uniprot.org) with the species restriction "Homo sapiens". GeneCards (http://www.genecards.org) provided Disease-related targets. The search keywords were "Chronic kidney disease" and "Kidney fibrosis", the category was "protein" and the species filter was "*Homo sapiens*".

Construction of protein-protein interaction (PPI) network and biological analysis. The corresponding targets of AE, CKD, and kidney fibrosis were plotted on the Venn to obtain the intersecting targets. Subsequently, we imported the potentially interacting targets into the String database (http://string-db.org/) and constructed a PPI network with the parameters "*Homo sapiens*", a minimum interaction score of 0.400, hiding unconnected points, and the rest of the parameters by default. Cytoscape software will be used to further analyze the PPI network, and the MCODE[23] plug-in will be used to perform the computational analysis of the nodes in the PPI network to filter out a subset of the most important ones (Degree Cutoff: 2; Node Score Cutoff: 0.2; K-Core: 2; Max Depth: 100).

To investigate the biological functions and biological pathways of the intersecting targets, Gene Ontology (GO) enrichment analysis was conducted using the Metascape database (http://www.metascape.org/) and Kyoto Encyclopedia of Genes and Genomes (KEGG) pathway analysis. The results were presented through the CNSknowall platform (https://cnsknowall.com). A p-value <0.05 was accepted.

Molecular docking

The PI3K protein crystal structure (PDB ID: 5DXT) was sourced from the RCSB PDB database (https://www.rcsb.org/) and the small molecule 3D structure was sourced from the PubChem database (https://pubchem.ncbi.nlm.nih.gov/). Docking was achieved through the utilization of blind docking on the CB-DOCK2 online server (https://cadd.labshare.cn/cb-dock2/php/blinddock.php).[24] The CB-DOCK2 system employs artificial neural networks for cavity probing and utilizes the Autodock Vina docking algorithm. All parameters of CB-DOCK2 are set to default, such as number of cavities for docking: 5. The results of the docking procedure will be selected based on the binding energy. Subsequent kinetic verification of binding stability will be conducted through force analysis and docking position assessment. Ligand-receptor force analysis was conducted with the aid of the PLIP online server (https://plip-tool.biotec.tu-dresden.de/plip-web), while the ligand-receptor 3D conformation was visualised using Pymol software.

In vivo study

Fifty 8-week-old male C57BL/6 mice (Viewsolid Biotechnologies, Beijing, China) were housed in specific pathogen-free (SPF) surroundings with 25°C temperature, 65% relative humidity and a 12 h light/dark cycle, and were allowed to access water and food *ad libitum*. After compliant feeding, the mice were randomly divided equally into five groups as follows: Control, Control+AE (20 mg/kg/day), adenine (50 mg/kg/day), AE10 (10 mg/kg/day), AE20 (20 mg/kg/day).[25] AE10 and AE20 were both administered in adenine were administered based on adenine. Adenine and AE were dissolved in purified water and 0.5% sodium carboxymethyl cellulose, respectively. Interventions

were carried out for 1 week, during which time mice were collected in urine and subsequently euthanized humanely, followed by blood and tissue samples.

Histopathology and immunohistochemistry

Kidney tissue specimens were fixed in 4% paraformaldehyde (Servicebio, Wuhan, China) overnight at 4°C, then dehydrated, cleared, and embedded in paraffin. Consecutive sections (2-5 μm thick) were cut.[26] For histology, sections underwent standard hematoxylin (G1004, Servicebio) and eosin (G1001, Servicebio) staining (H&E) and Masson's trichrome staining (G1006 kit, Servicebio) following established protocols.[27] For immunohistochemistry (IHC), deparaffinized sections underwent antigen retrieval (citrate buffer, pH 6.0, 95°C, 20 min), endogenous peroxidase blocking (3% H_2O_2, 15 min, RT), and blocking (5% BSA, 30 min, RT). Sections were incubated overnight at 4°C with primary antibodies: Fibronectin (Rabbit polyclonal, 1:1500, GB114491-100, Servicebio) and Collagen I (Rabbit polyclonal, 1:1000, GB11022-3-100, Servicebio). Negative controls used PBS instead of primary antibody. After washing, sections were incubated with HRP-conjugated Goat Anti-Rabbit IgG secondary antibody (1:200, GB23303, Servicebio) for 50 min at RT. Signal was visualized with DAB (G1211-200T, Servicebio) followed by nuclear counterstaining with Mayer's haematoxylin (G1004, Servicebio) for 1 min. Negative controls were conducted by omitting the primary antibody to ensure specificity of the staining. Slides were dehydrated, cleared, mounted, and examined under a light microscope (BX53, Olympus; Tokyo, Japan) with a 40x objective.[28] For each sample, three randomly selected fields were analyzed to ensure representative data. Image analysis was conducted using ImageJ software to quantify the percentage of positively stained cells. Three randomly selected fields per sample were analyzed, and the average percentage of immune-positive cells was reported.

Cell culture and treatment

HK-2 cells were cultured in Dulbecco's Modified Eagle's Medium (DMEM)/F-12 containing 10% foetal bovine serum (FBS, CellMax, Australia) and 1% penicillin/streptomycin, in an incubator at 37°C and 5% CO_2. TGF-β1 (10 ng/ml) induced HK-2 cells as an *in vitro* model of renal fibrosis. Then, the cells were treated with different levels of AE (CAS: 418-72-1, purity >98.0%, cat: SA8200, Solarbio Science & Technology, Beijing, China) and 740Y-P (30 μM, MCE, Monmouth Junction, NJ, USA) for 24 h.[29]

Cell proliferation assay

The effect of AE on TGF-β1-induced proliferation of HK-2 cells was assessed utilizing the Cell Counting Kit-8 (CCK-8) according to the instructions. 1×10^5 HK-2 cells were inoculated into each well of a 96-well plate and waited until the cells were attached to the wall, then different concentrations of AE were added to treat the TGF-β1-induced cells. After this, add 10 μL of CCK-8 solution and keep for 1 h. Cell proliferation was analyzed according to the results measured by the zymography (450 nm). Furthermore, the results were replicated 8 times for each concentration.

Plasmid and siRNA transfection of cells

The coding sequence of PIK3CA was cloned into the pcDNA3.1 vector (Beyotime, Shanghai, China). The structure of the specific locus was changed using a rapid mutation system. Transfect the plasmid using the liposomal lip3000 method. Ensure that the cells are 70-80% covered in the 6-well plate before the experiment. Heat the DMEM water bath at 37°C and place the transfection reagents and DNA plasmid at room temperature. Prepare two centrifuge tubes, add 125 μL DMEM to each tube, add lipofectamine 3000 μL to tube 1, and incubate at room temperature for 5 min; 2.5 μg DNA plasmid was added to tube 2 and the two centrifuge tubes were mixed and left to stand at room temperature for 5 min. When the DNA liposomes were left to stand for 4 min, HK-2 cells to be transfected were taken out from the 37°C incubator, and the DNA liposomes were incubated with DMEM. C incubator, gently over-washed with DMEM and then added DMEM 1.5 mL/well. When the time was up, 0.25 mL of DNA-liposome mixture was added drop by drop into the culture dish, and the dish was incubated in the incubator at 37°C with 5% CO_2 for 4-6 h, then changed to 10% FBS-DMEM culture medium, and continued to incubate for 48 h to establish a stable cell line. PI3K (siRNA) was transfected into cells *via* Liposome 3000 (Mei5 Biotechnology; Beijing, China). The target sequences[30] were sense 5′-GCUAUCCUCUGAACAACUATTdTdT-3′ and antisense 5′-UAGUUGUUCAGA GGAUAGCTTdTdT-3′.

Immunofluorescence

Pre-treated tissues and cells were incubated overnight at 4°C with primary antibodies, anti-P-Pi3k (1:100,17366S, Cell Signaling Technology, Danvers, MA, USA), anti-Pi3k (1:100, ab278545, Abcam, Cambridge, MA, USA), anti-Akt (1:200, 4691S, Cell Signaling Technology), anti-P-Akt (1:400, 4060S, Cell Signaling Technology), anti-GSK3β (1:200, K000041M, Solarbio) and anti-P-GSK3β (1:100, GB114582-100, Servicebio). The fluorescent secondary antibodies (1:800GB25301/GB28301, Servicebio) were added to the samples in a light-avoiding environment and incubated for 2 h at room temperature in the absence of light. Finally, DAPI (10 μg/mL) was incubated away from light for 5 min. Negative controls were conducted by omitting the primary antibody to ensure specificity of the staining. Immunofluorescence results were acquired through the use of laser confocal microscopy (LSM800, Zeiss, Oberkochen, Germany) in a 40x objective. Image analysis was performed using ImageJ software (National Institutes of Health). The precise methodology employed for immunofluorescence was consistent with that previously described.[31] All experiments were repeated three times.

Western blotting assay

This experiment was performed using α-SMA (1:1000, 19245S, Cell Signaling Technology), Vimentin (1:1000, ab92547, Abcam), PI3k (1:100, sc-365290, Biotechnology, Santa Cruz, CA, USA), P-Pi3k (1:1000, ab278545, Abcam), GSK3β (1:1000, K000041M, Solarbio, Beijing, China), P-GSK3β (1:300, GB114582-100, Servicebio), Akt (1:1000, 4691S, Cell Signaling Technology), P-Akt (1:1000, 4060S, Cell Signaling Technology) and β-actin (1:10,000, sc-47778, Santa Cruz Biotechnology) antibodies. Specific signals were detected using a gel imaging system program (iBright CL1000, Thermo Fisher Scientific, Waltham, MA, USA), and the above signals were analyzed using Image J software. Specific steps were performed according to the previously described.[32]

Statistical analysis

All data are expressed as mean ± SEM values. To analyze the data, multiple comparisons were performed using ANOVA (one-way analysis of variance) and Dunnett's *t*-test. A *p*-value of less than 0.05 was deemed to be statistically significant. The data were evaluated with the use of GraphPad Prism version 8.0 (GraphPad Prism Software, La Jolla, CA, USA).

Results

Acquisition of target points and construction of the PPI network

We obtained 23 biomolecular targets of AE and explored the chemical structure of AE in depth with the help of the PubChem database and KingDraw, obtaining Figure 1A. For CKD and renal fibrosis biomolecular targets, we obtained 12,850 and 7,975 respectively. By comparing the data of related proteins in three groups, we identified 21 common proteins (Figure 1B). With the help of the STRING database, we created a PPI network of the intersection proteins (Figure 1C). This network comprises 21 nodes, 75 edges, an average node degree of 7.14, and a local clustering coefficient of 0.676. The MCOD analysis of the PPI network conducted with Cytoscape software revealed the most core clustered sub-network, including CASP3, TP53, PTGS2, HSP90AB1, PIK3CA, IL1B, PRKCD, CDC42, TNF, MYC, and BAX, as shown in Figure 1D.

Enrichment analysis

To gain insight into the potential biological processes that AE may induce in renal fibrosis, the identified common genes were further analyzed. The GO analysis unveiled three main categories: biological processes (BP), cellular components (CC), and molecular functions (MF). Major biological processes include positive regulation of lipid catabolic process, programmed necrotic cell death, and positive regulation of an acute inflammatory response. Principal molecular functions identified were cytokine receptor binding, kinase regulator activity, protein kinase regulator activity, protease binding, and protein serine kinase activity. The primary cellular components involved were the nuclear periphery, neuronal cell body, cell body, transferase complex, *etc*. (Figure 1E). In furthermore, the top twenty pathways shown in Figure 1F were confirmed by KEGG enrichment analysis. It was found that eight signaling pathways, including the AGE-RAGE signaling pathway in diabetic complications, IL-17 signaling pathway, NF-kappa B signaling pathway, PI3K-Akt signaling pathway, VEGF signaling pathway, chemokine signaling pathway, hepatitis B, and human

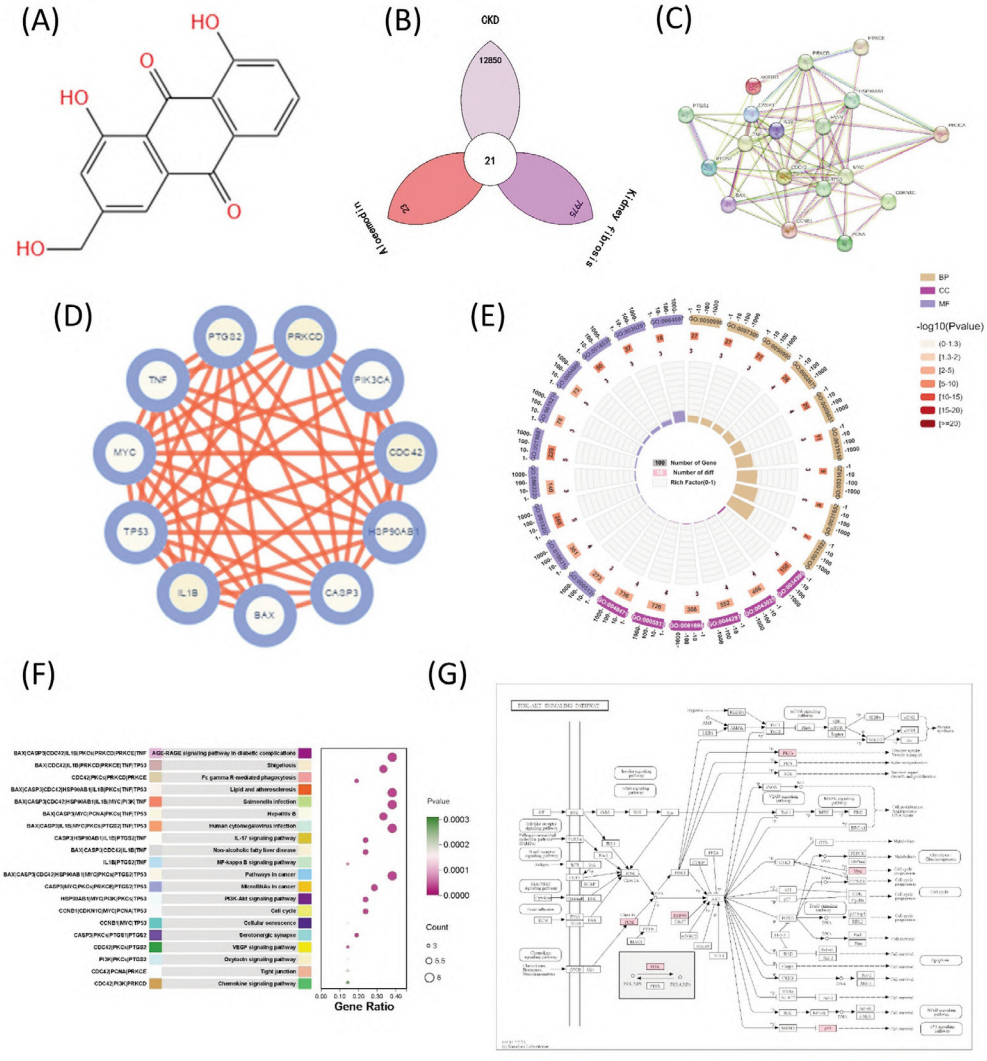

Figure 1. Network pharmacological analysis of aloe-emodin-associated proteins in CKD fibrosis. **A**) Structure of aloe-emodin. **B**) Venn diagram of overlapping proteins between CKD, kidney fibrosis and aloe-emodin related target genes. **C**) PPI network of overlapping target genes. **D**) PPI network key subset. **E**) GO enrichment analysis of predicted targets of overlapping proteins. **F**) KEGG analysis of predicted proteins of overlapping proteins. **G**) KEGG Diagram hsa04151.

cytomegalovirus infection, play key roles either directly or indirectly in the occurrence and development of inflammation and fibrosis. Therefore, it is highly likely that AE can improve the progression of renal fibrosis through the aforementioned pathways.

By utilizing the KEGG database to identify and screen the obtained signaling pathways, we discovered the PI3K-Akt signaling pathway that controls various biological reactions within cells (Figure 1G). GSK3β is identified as one of its key downstream molecules. It has been reported that multiple AKT pathways are activated in lung fibrosis models,[33] including the activation of the AKT/GSK3β signaling pathway in bronchial epithelial cells induced by bleomycin.[34] Based on these analyses, we selected the PI3K/Akt/GSK3β signaling pathway to verify the preventive and therapeutic effects of AE on kidney fibrosis.

AE alleviates renal function, renal pathologic changes and renal fibrosis in adenine-induced mice

To evaluate the effect of AE on adenine-induced kidney injury in mice, we conducted oral administration of drugs to the mice for one week. The findings of the experimental study demonstrated that, in comparison to the adenine model group, the AE treatment

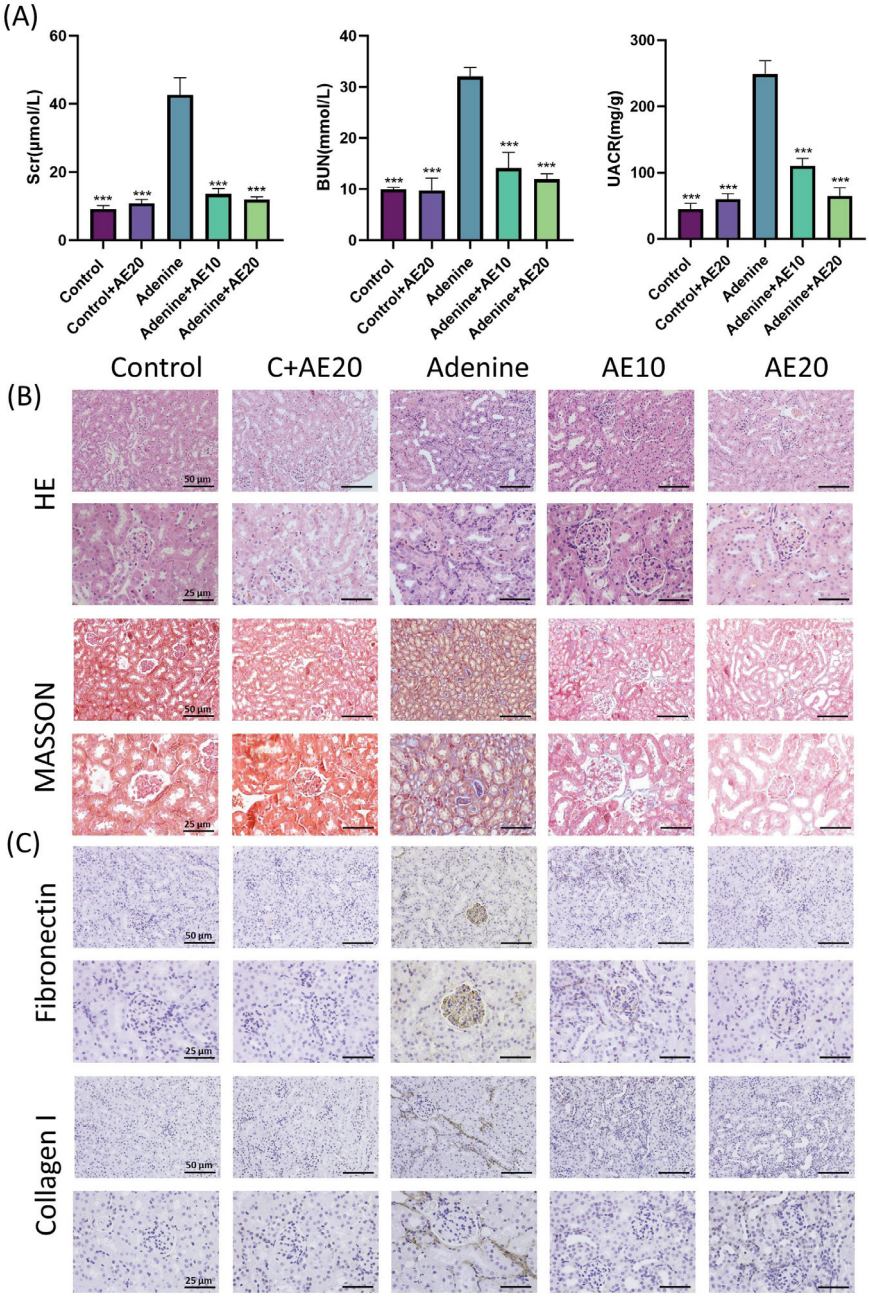

Figure 2. The effect of AE in adenine-induced mice. **A**) MOR improve the level of Scr and BUN in blood; decreased the level of UACR in urine. **B**) H&E staining reflects the extent of kidney damage in mice after 7 days of AE treatment; Masson's trichrome staining shows the extent of collagen fibril deposition in mice after 7 days of AE treatment. **C**) Immunohistochemical staining showed expression of fibronectin and collagen I after 7 days of AE treatment. Data are expressed as mean ± SD. n=10, *p<0.05; **p<0.01, ***p<0.001 compared with the model group.

regimen resulted in a notable reduction in serum creatinine (Scr), blood urea nitrogen (BUN) levels, and urine albumin/creatinine ratio (UACR), but there was no statistical difference between the high and low dose groups (Figure 2A). In Figure 2B, H&E staining showed glomerular swelling in the model group, and inflammatory cell infiltration in the kidney interstitial area; collagen fiber deposition was evident in kidney tissue sections stained with Masson's trichrome. By comparison, the kidney tissue pathology of the AE group was good. In addition, we performed IHC on the kidneys of the mice. The experiments showed that fibronectin and collagen I were widely deposited in the ECM of adenine mouse kidneys, and the addition of AE reversed the situation of kidney fibrosis (Figure 2C). Further analysis has shown that AE can be effective in decreasing the degree of glomerulosclerosis and interstitial fibrosis, and has a significant alleviating effect on adenine-induced kidney function damage and pathological changes in the kidney.

AE interferes with the PI3K/AKT/GSK3β signaling pathway in adenine-induced mice and ameliorates renal fibrosis

Network pharmacology revealed the potential mechanism of AE's effect on the kidney. We noted through immunofluorescence

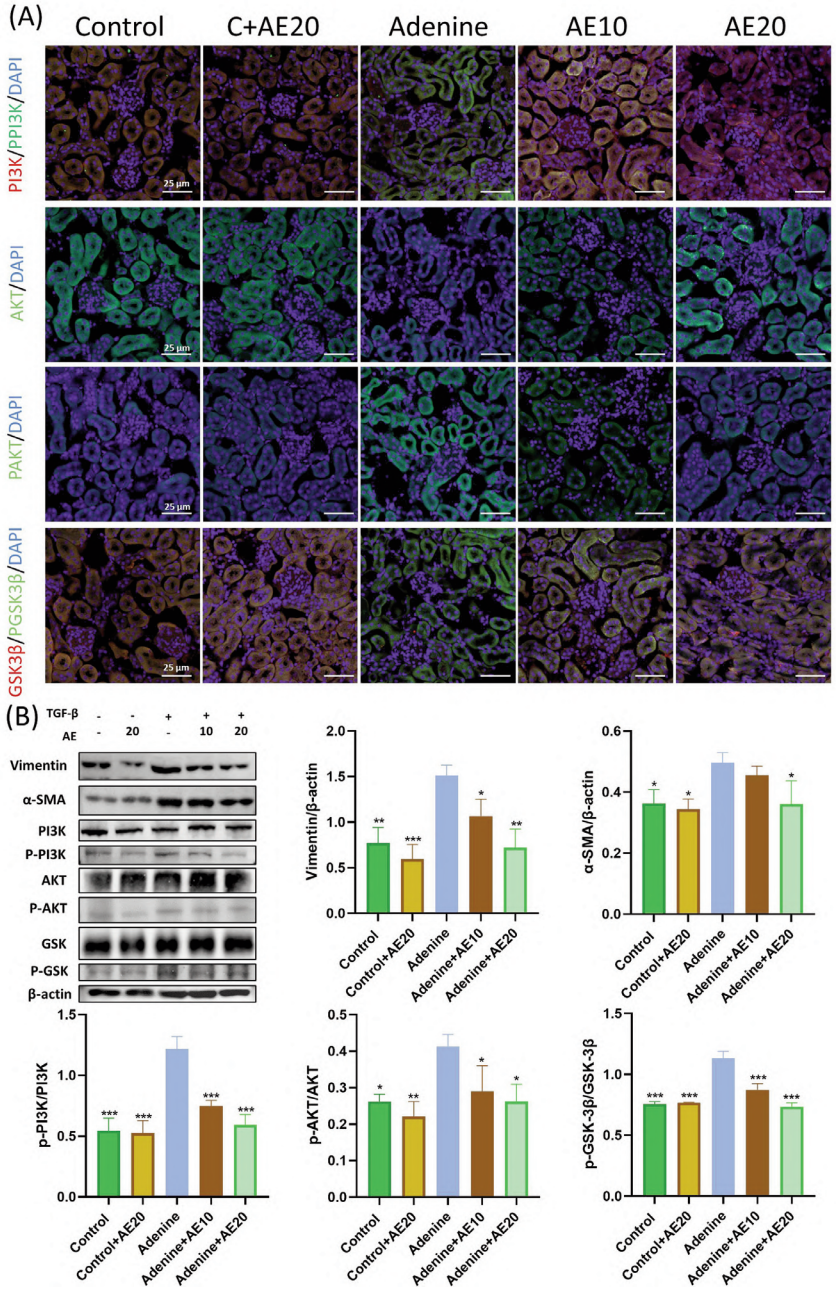

Figure 3. Regulation of PI3K/AKT/GSK3β pathway by AE in adenine-induced mice. **A**) Immunofluorescence staining of p-PI3K, PI3K, p-Akt, Akt, p-GSK3β and GSK3β in Adenine-induced mice after 7 days of AE treatment. **B**) Protein expression levels of p-PI3K/PI3K, p-Akt/Akt, p-GSK3β/GSK3β, Vimentin and α-SMA in each specific group of mice after 7 days of AE treatment. *p<0.05; **p<0.01, ***p<0.001 compared to the KKAy group.

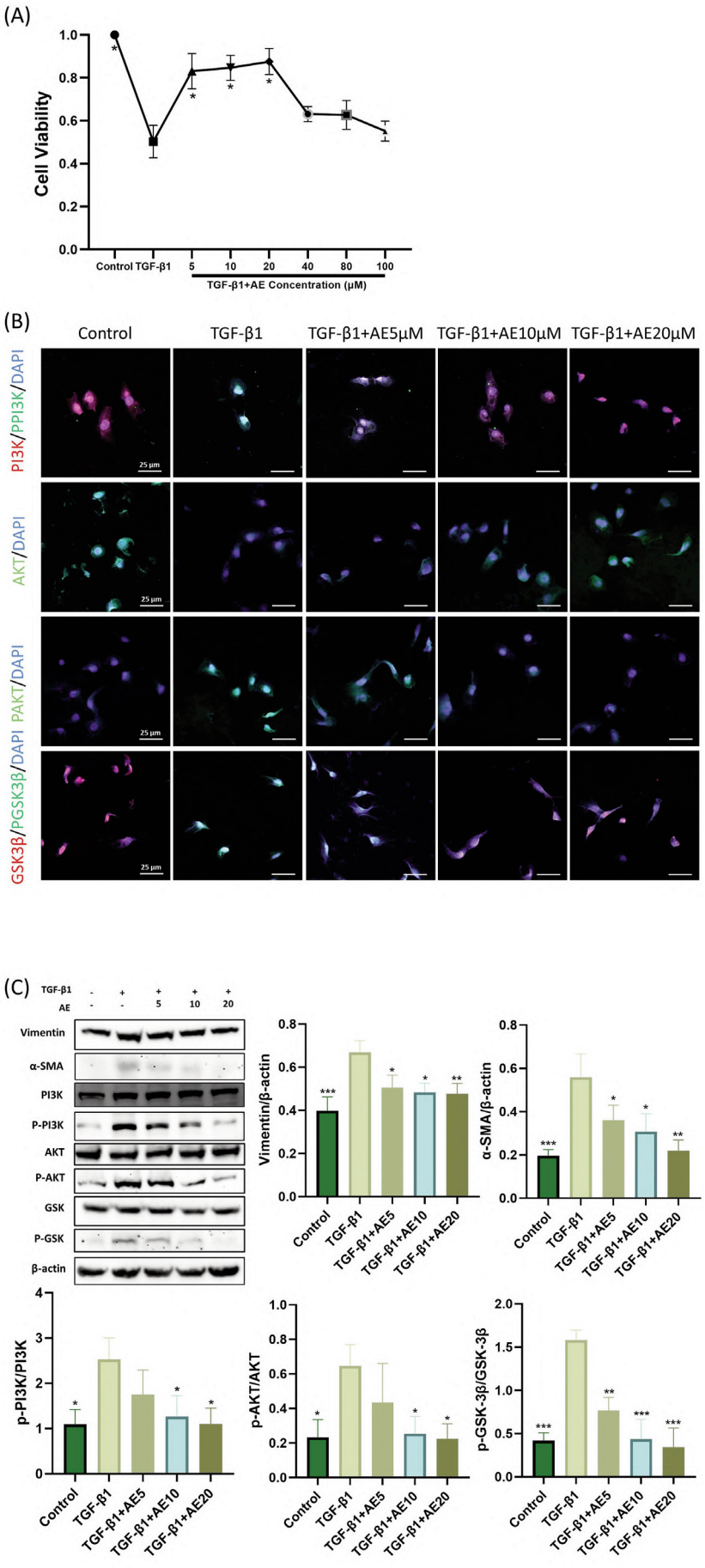

Figure 4. AE improving renal fibrosis by inhibiting the PI3K/AKT/GSK3β signaling pathway in TGFβ-1-stimulated HK-2 cells. **A**) The effect of AE on the proliferation of HK-2 cells. **B**) Immunofluorescence staining of p-PI3K, PI3K, p-Akt, Akt, p-GSK3β and GSK3β for each specific group. C) Protein expression levels of p-PI3K/PI3K, p-Akt/Akt, p-GSK3β/GSK3β, vimentin and α-SMA in each specific group of HK-2 cells. *p<0.05; **p<0.01, ***p<0.001 compared to TGFβ-1 group.

staining that the expression of phosphorylated PI3K, AKT, and GSK3β increased significantly in the kidney tissues of adenine mice. However, in the AE group, their expression levels were significantly reduced, close to the level of the control group (Figure 3A). Fortunately, our protein immunoblotting results were in line with this observation, showing significant increases in the ratios of p-PI3K/PI3K, p-Akt/Akt, and p-GSK3β/GSK3β (Figure 3B). Notably, the protein levels of the fibrotic molecules vimentin and α-SMA were also significantly increased in the adenine group and dramatically reduced after AE treatment. However, increasing the dose of AE did not seem to significantly improve its therapeutic effect, with no statistical significance. The above results imply that AE may improve kidney fibrosis by inhibiting the activation of the PI3K/AKT/GSK3β signaling pathway, which is likely related to the regulation of epithelial-mesenchymal transition.

AE inhibits PI3K/AKT/GSK3β signaling pathway activation and ameliorates TGF-β1-induced fibrosis in HK-2 cells

In order to clarify the potential mechanism of AE, we chose cell models for *in vitro* experiments to verify its anti-fibrotic effect. The results in Figure 4A show that compared to the TGF-β1 group,

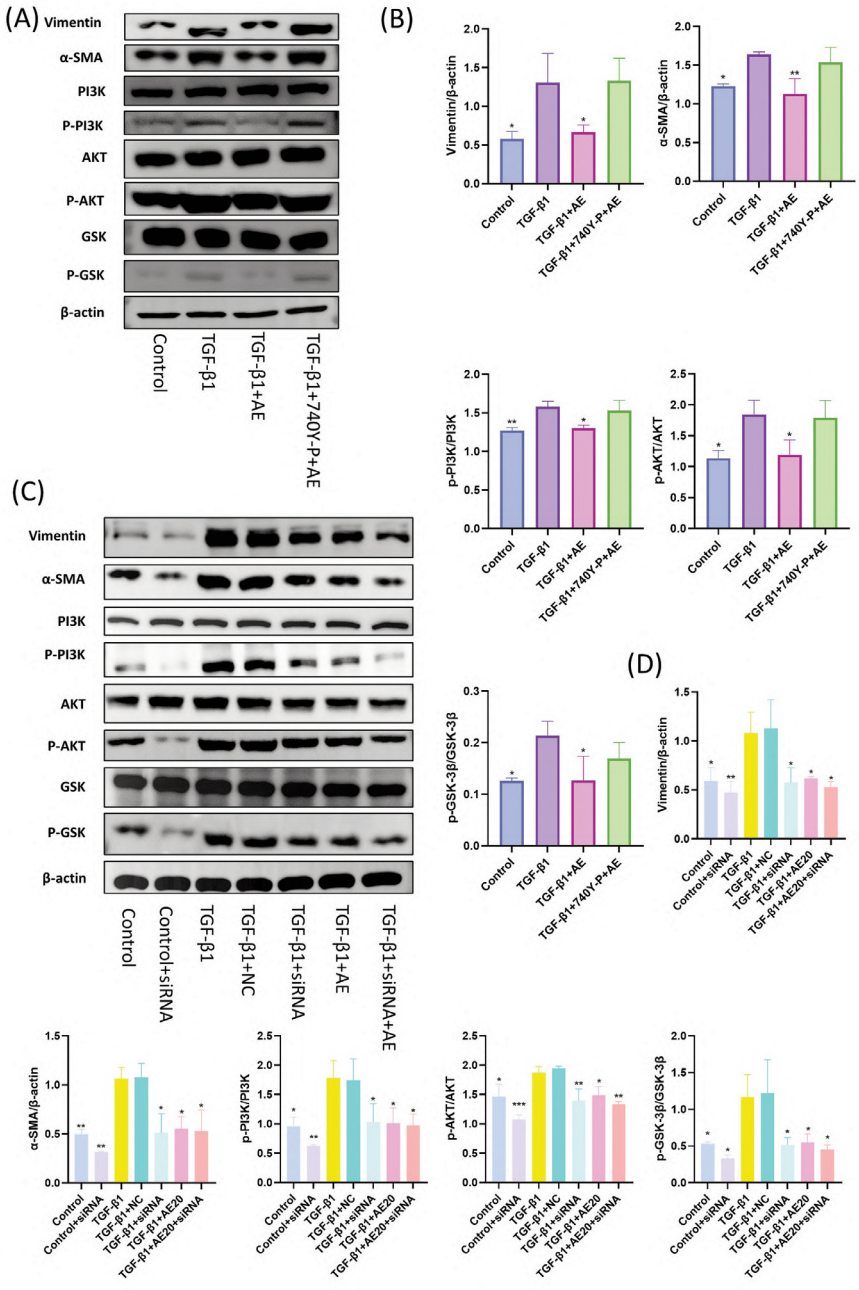

Figure 5. Inhibition and activation of PI3K alters fibrosis in HK-2 cells. **A**) Protein levels of p-PI3K, PI3K, p-Akt, Akt, p-GSK3β, GSK3β, vimentin and α-SMA in HK-2 cells in each group after 740Y-P treatment. **B**) Protein expression levels of p-PI3K/PI3K, p-Akt/Akt, p-GSK3β/GSK3β, Vimentin and α-SMA in each specific group of HK-2 cells. **C**) Protein levels of PI3K, p-Akt, Akt, p-GSK3β, GSK3β, vimentin and α-SMA in each group after PI3K silencing. **D**) Levels of p-PI3K/PI3K, p-Akt/Akt, p-GSK3β/GSK3β, vimentin and α-SMA. **p*<0.05; ***p*<0.01, ****p*<0.001 compared to TGFβ-1 group.

cell viability increased significantly with various doses of AE, and the intervention concentrations of 5 μM, 10 μM, and 20 μM worked the best. Therefore, these concentrations were used in subsequent experiments. First, we conducted immunofluorescence experiments. The experiment results show that changes in PI3K, AKT, and GSK3β in TGF-β1-induced HK-2 cells were consistent with those in adenine mouse kidneys (Figure 4B). In Western blot experiments, we observed the changes of vimentin and α-SMA in HK-2. The stimulation of TGF-β1 increased the expression of these proteins, intensifying the fibrosis of HK-2 cells. At the same time, PI3K was activated in HK-2. The ratio of p-PI3K/PI3K was highest in the model group, and then AKT and GSK3β were also activated (Figure 4C). All the above conditions were inhibited after AE treatment. These changes reveal that AE delays the fibrosis process of TGF-β1-induced HK-2 cells by inhibiting the activation of the PI3K/AKT/GSK3β signaling pathway.

Inhibition and activation of PI3K alters fibrosis in HK-2 cells

To further elucidate the role of AE and PI3K/AKT/GSK3β signaling pathways in HK-2 cell fibrosis, we performed more in-depth experiments. First, we used the cell-permeable PI3K activa-

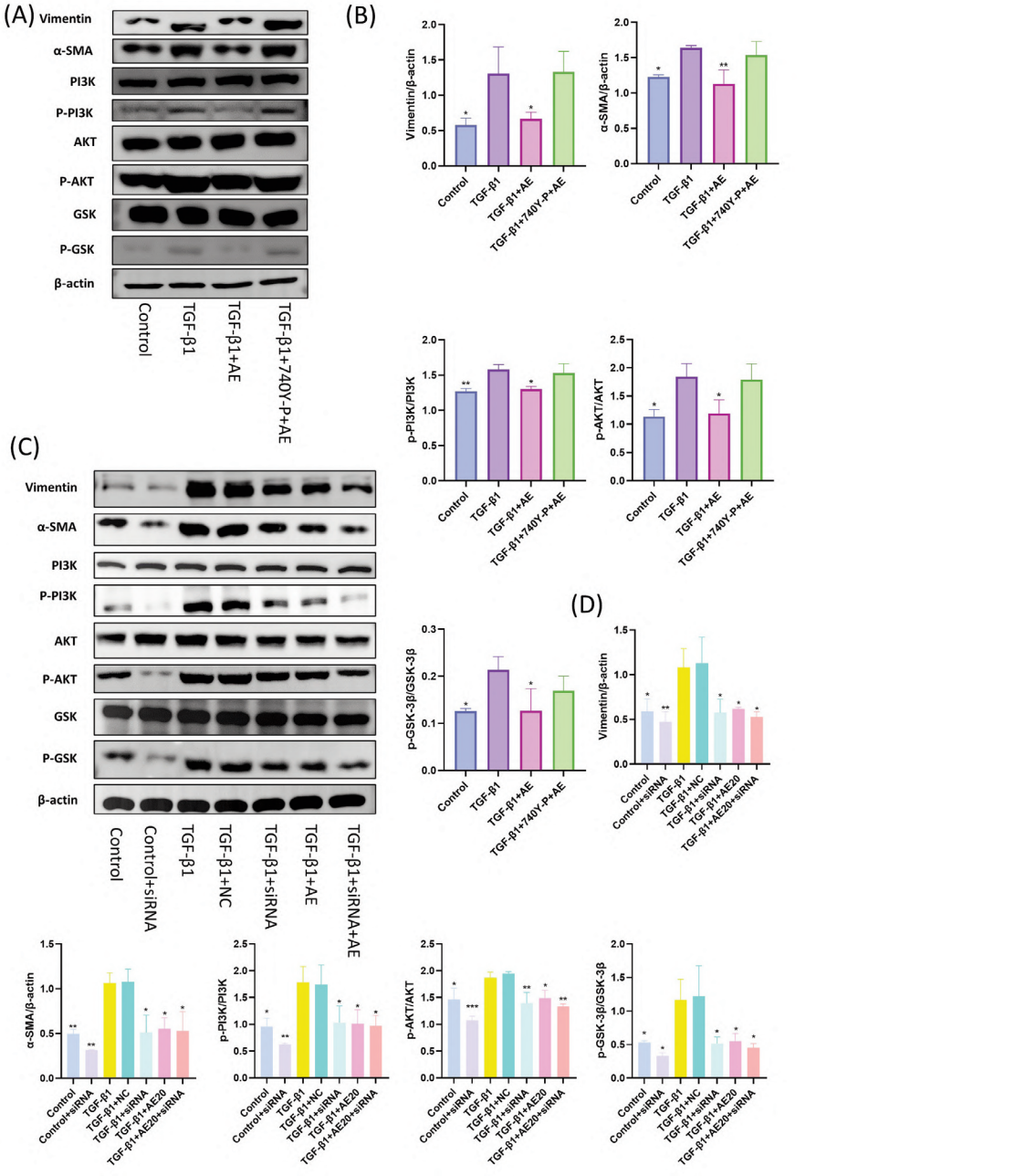

Figure 5. Inhibition and activation of PI3K alters fibrosis in HK-2 cells. **A**) Protein levels of p-PI3K, PI3K, p-Akt, Akt, p-GSK3β, GSK3β, vimentin and α-SMA in HK-2 cells in each group after 740Y-P treatment. **B**) Protein expression levels of p-PI3K/PI3K, p-Akt/Akt, p-GSK3β/GSK3β, Vimentin and α-SMA in each specific group of HK-2 cells. **C**) Protein levels of PI3K, p-Akt, Akt, p-GSK3β, GSK3β, vimentin and α-SMA in each group after PI3K silencing. **D**) Levels of p-PI3K/PI3K, p-Akt/Akt, p-GSK3β/GSK3β, vimentin and α-SMA. *p<0.05; **p<0.01, ***p<0.001 compared to TGFβ-1 group.

tor 740Y-P. As shown in Figure 5 A,B, the PI3K/AKT/GSK3β signaling pathway was fully activated and the levels of vimentin and α-SMA was significantly upregulated in the fibrosis model cells; when 740Y-P and AE stimulated fibrosis model cells simultaneously, in terms of protein expression, AE counteracted the effect of 740Y-P in activating PI3K and inhibited PI3K activation. This suggests that AE may regulate PI3K/AKT/GSK3β signaling pathway transduction and attenuate cellular fibrosis by inhibiting PI3K activation. We then transfected the siRNA of PI3K into HK-2 cells to silence its expression. In Figure 5 C,D we can see that the ratio of p-PI3K/PI3K was significantly reduced after silencing compared to the control group, as was the expression of p-Akt/Akt and p-GSK3β/GSK3β. The differences between the TGF-β1 and TGF-β1+NC groups were not statistically significant. In addition, in comparison to the model group, the TGF-β1+siRNA group demonstrated a notable reduction in the levels of Vimentin and α-SMA, which was consistent with the results of the AE group. Nevertheless, in the TGF-β1+siRNA+AE group, the superimposition of these two elements did not have a one-plus-one effect. The above results suggest that activation of PI3K promotes the progression of fibrosis, whereas inhibition of PI3K attenuates cellular fibrosis. When HK-2 cells received AE treatment, AE could slow down the fibrotic progression of the cells by inhibiting the activation of PI3K and thus modulating the PI3K/AKT/GSK3β signaling pathway.

AE exerts fibrosis inhibition by binding to specific sites of PI3K

In the present study, molecular docking experiments were conducted to confirm the mechanism of action of AE and PI3K. On docking, it was observed that a specific interaction had been formed between AE and PI3K. The binding energy between ligand and receptor was calculated to be -9.0 kcal/mol using the Vina binding energy prediction algorithm based on the AMBER force field. The protein-ligand-formed complexes were analyzed for interaction forces relying on the PLIP server and the results were subsequently presented using the molecular modelling software Pymol. In Figure 6A, we have labelled a certain number of hydrogen bonds formed by proteins with the carboxyl groups of the compounds in red and those interacting with the π-π stack in orange, and have labelled specific interacting residues in the figure with the corresponding bond lengths in angstroms next to the dashed lines. Concurrently, the analysis of the ligand-protein mutual position, when considered in conjunction with the overall analysis,

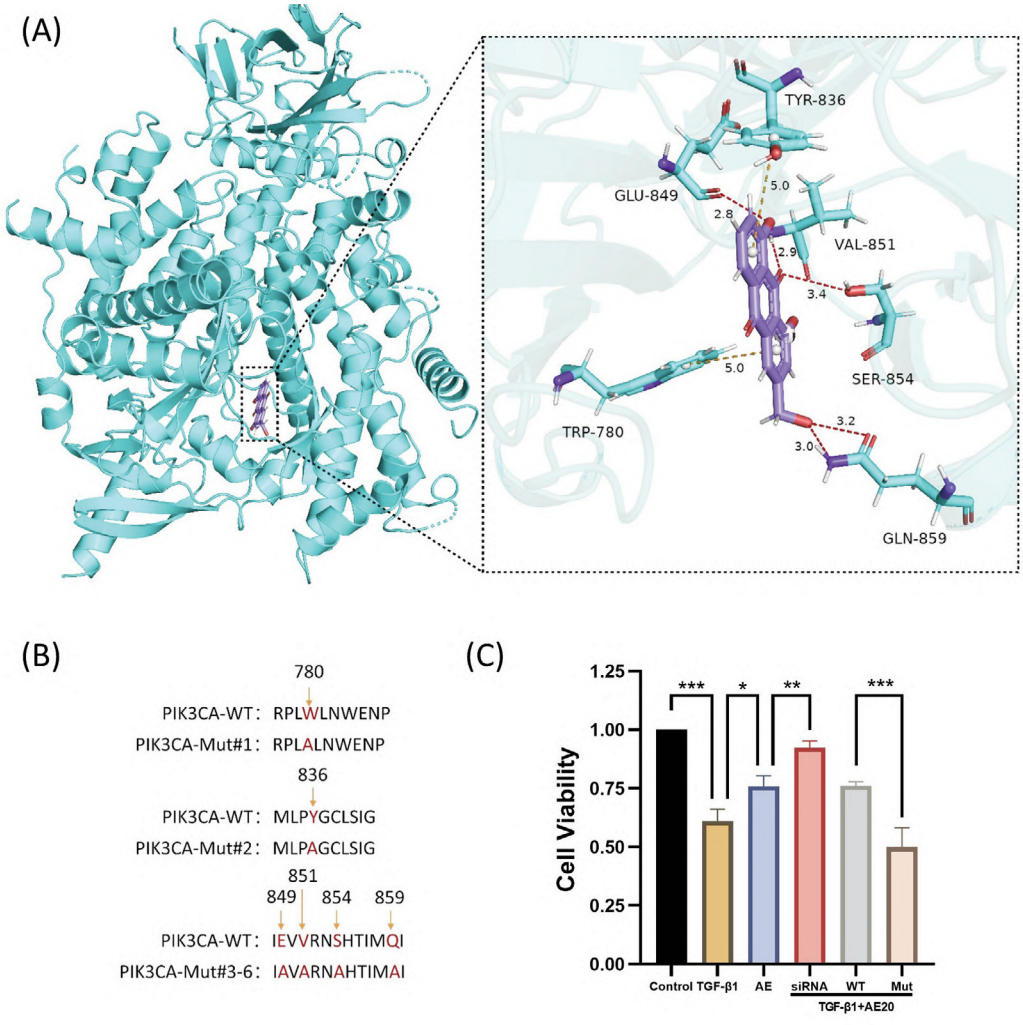

Figure 6. AE inhibits fibrosis by binding to PI3K. **A**) Predicted homology modelling structure of AE and PI3K protein binding site. **B**) Schematic diagram of PI3K mutation. **C**) PI3K-deficient HK-2 cells were re-expressed using the overexpressed plasmid, treated with AE for 24 h, and detected by CCK-8. *p<0.05; **p<0.01, ***p<0.001 compared to TGFβ-1 group.

reveals that the ligand binds to the internal cavity of the protein with low free energy, forming a specific number of hydrogen bonds and a range of interactions. It can be postulated that the ligand and the receptor form a more stable complex.

On this basis, we constructed plasmids for PI3K mutants, which included TRP-780, TYR-836, GLU849, VAL-851, SER-854 and GLN-859 (Figure 6B). To establish PI3K-deficient HK-2 cells, we overexpressed with wild-type PI3K and mutant PI3K and treated with TGF-β1 and AE, respectively. The results of the CCK-8 assay showed that wild-type PI3K significantly restored the reduced cellular activity of TGF-β1 when stimulated by AE. However, PI3K-deficient HK-2 cells caused by mutant PI3K did not increase HK-2 cell activity after TGF-β1 and AE stimulation, suggesting reduced sensitivity to AE (Figure 6C). Thus, AE can only exert its therapeutic effect by binding to specific sites of PI3K. Taken together, the results of previous experiments lead to the conclusion that AE inhibits the activity of PI3K by binding to it and ameliorates renal fibrosis by modulating the PI3K/AKT/GSK3β signaling pathway.

Discussion

CKD is a condition characterized clinically by a gradual deterioration in renal function. The underlying causes of CKD are numerous and diverse, including diabetes and hypertension.[35] The typical lesion is a gradual covering of healthy renal cells with ECM proteins, resulting in renal fibrosis.[36] However, no drugs have been approved to specifically target and directly treat renal fibrosis. Indirectly addressing renal fibrosis by controlling the progression of CKD is currently the dominant solution, including the use of standard medications such as ACE inhibitors, angiotensin II receptor blockers (ARBs) to control the causes of renal damage, and strict glycemic control in diabetic patients.[37] The identification of effective new strategies for the treatment of kidney fibrosis is therefore of great importance. The results of recent research indicate that the active ingredients of Chinese medicines may have potential antifibrotic effects,[38,39] which reveals that we may be able to discover effective anti-renal fibrosis drugs from the wealth of Chinese medicinal resources.

AE, scientifically known as 1,8-dihydroxy-3-(hydroxymethyl) anthraquinone, with a chemical molecular formula of $C_{15}H_{10}O_5$ and a relative molecular mass of 270.23, is an anthraquinone compound extracted from the roots and rhizomes of rhubarb.[40] A number of biological properties and potential therapeutic benefits have been ascribed to AE.[8] Nevertheless, the impact of AE on renal fibrosis in CKD patients remains to be determined. Using network pharmacology and basic experiments, we predicted and assessed putative AE proteins and signaling pathways against kidney fibrosis. It was revealed that AE may attenuate renal fibrosis by inhibit-

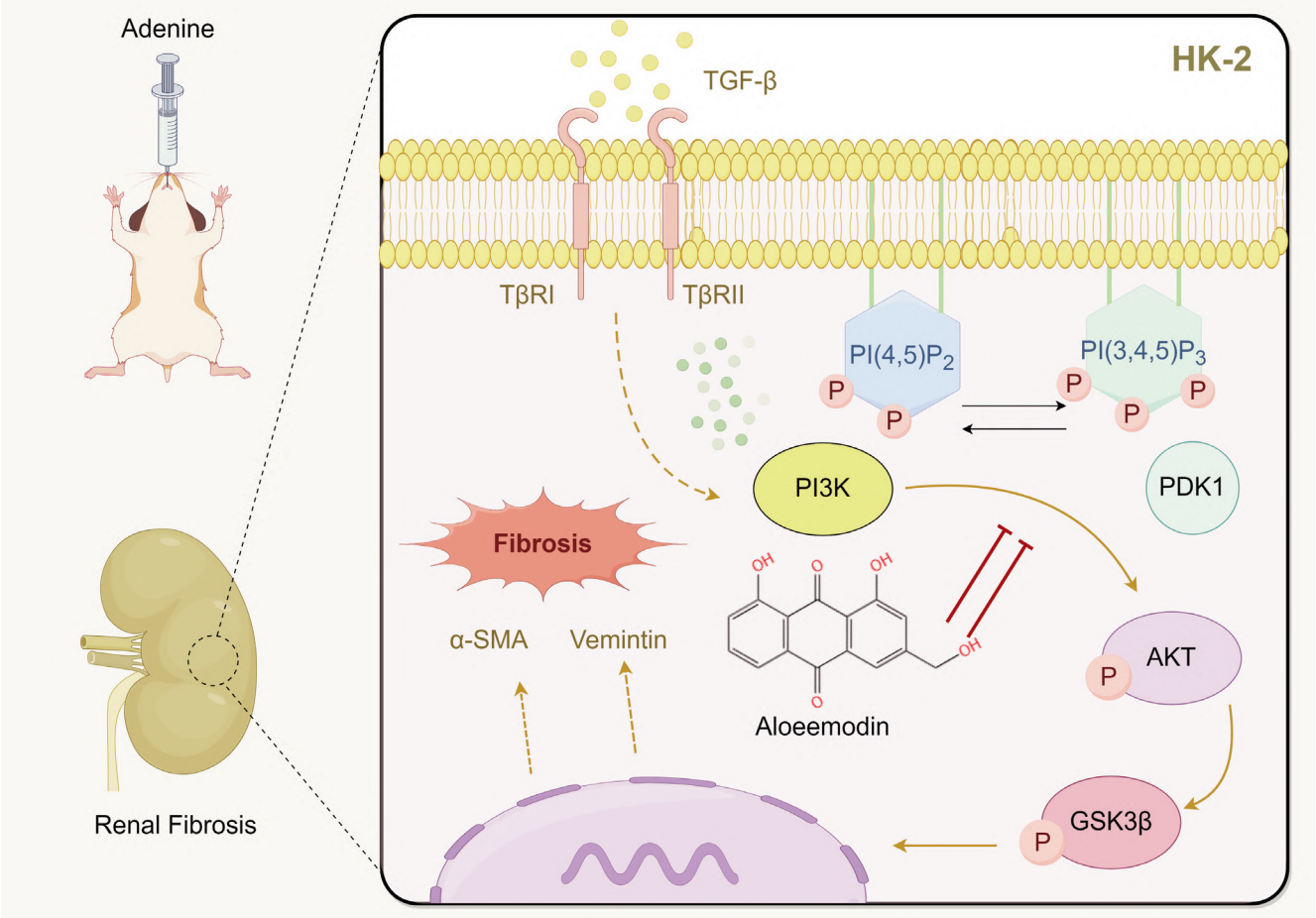

Figure 7. Schematic summary of AE amelioration of renal fibrosis through inhibition of the PI3K/AKT/GSK3β signaling pathway.

ing the PI3K/Akt/GSK3β signaling pathway (Figure 9 C-F). *In vivo* and *in vitro* analyses showed that Aloe vera rhodopsin had an inhibitory effect on kinase activity and the corresponding molecules, which is consistent with the findings of Dou *et al.*[25]. The consistency between the different models emphasizes the therapeutic role of AE through this pathway, which coincides with the study by Liang *et al.*[41] and Cheng *et al.*,[42] which provides a good basis for combating the progression of chronic renal failure.

During the experiments, we proved for the first time that AE had an antifibrotic effect and protected against renal injury using adenine-induced CKD mice. AE ameliorated histopathological abnormalities in model mice (Figure 1), reduced collagen staining area and mesangial cell proliferation, and attenuated Scr, BUN, and UACR. Also, IHC showed that AE diminished the expression of fibrotic proteins, including fibronectin and collagen I, in the kidneys of adenine mice. Fibronectin and collagen I are two key ECM proteins, and the extent to which they are deposited in the kidney is directly correlated with damage to kidney structure and function.[43] Notably, back in 2019, Cai *et al.* demonstrated that AE significantly inhibited human hepatic stellate cell proliferation and affected apoptosis,[44] and that the activation and proliferation of hepatic stellate cells played a central role in the process of liver fibrosis.[45] Recent research evidence increasingly suggests that epithelial-mesenchymal transition (EMT) is a crucial factor in the development of renal fibrosis, as transformed epithelial cells exacerbate the fibrotic process by secreting ECM proteins.[46] Meanwhile, some scholars have found that AE can inhibit and reverse EMT in a variety of cancer cells,[47,48] which makes us wonder whether AE can similarly inhibit or reverse EMT in renal tubular epithelial cells, or even reverse the process of renal fibrosis. Importantly, our study validated the capability of AE to decrease the expression of the EMT marker protein vimentin,[49] attenuate kidney injury, and inhibit renal fibrosis. Furthermore, the specific molecular mechanism of its effect was analyzed through network pharmacology and molecular docking, and the close association of AE with the PI3K/Akt/GSK3β signaling pathway was verified. The PI3K/AKT signaling pathway is of pivotal importance in the study of fibrosis, and there is an increasing recognition of its contribution to the fibrosis process. The reviews by Wang *et al.* [50] and Qin *et al.*[51] summarized and reported the findings of the PI3K/AKT pathway in idiopathic pulmonary fibrosis and cardiac fibrosis, respectively, and concluded that PI3K/AKT is a key signaling node during fibrosis, with potential significance for the development of novel antifibrotic strategies. In renal disease, a study by Liu *et al.*[52] found that Paeoniflorin was able to inhibit the proliferation and cell cycle progression of human mesenchymal cells (HMCs) and reduce the level of inflammatory factors and iNOS expression. In addition, the compound strongly inhibited the PI3K/AKT/GSK3β pathway and potentiated the effects of PI3K inhibitors, while also resisting the activating effect of insulin-like growth factor 1 (IGF-1) on this pathway. GSK3β is a key downstream signaling molecule of AKT, influencing inflammation and fibrosis.[53,54] In addition, GSK3β may represent a promising therapeutic target for renal fibrosis.[55] These findings suggest that the PI3K/AKT/GSK3β signaling pathway inhibits the activation and differentiation of HMCs and reduces the deposition of ECM, *e.g.*, collagen I, fibronectin, *etc*.,[56] thereby inhibiting fibrosis formation. The results of these analyses are in perfect agreement with our experimental performance. In the present experiments, we found that AE not only inhibited adenine-induced renal injury in mice and attenuated the expression of the fibrosis indicators vimentin and α-SMA, but also inhibited the overexpression of the PI3K/AKT/ GSK3β pathway in an *in vivo* model (Figure 3). Notably, Dou *et al.* reported similar findings, confirming that inhibition of this signaling cascade by AE plays a key role in ameliorating renal fibrosis.[25] More importantly, a series of functional analyses based on molecular docking data showed that AE failed to exert antifibrotic activity in PI3K-deficient HK-2 cells (Figure 6). As illustrated in the graph, the survival of HK-2 was decreased after TGF-β1 treatment, but cell survival was improved after AE treatment (Figure 6C). However, when the cells were treated with plasmid, the protective effect of AE on HK-2 lost its effect and cell survival decreased. The analysis of these results suggests that AE inhibits the activity of PI3K mainly by binding to PI3K, thus protecting renal function and improving fibrosis. Furthermore, the results indicate that PI3K may serve as a promising target for therapeutic intervention in the management of renal fibrosis.

Furthermore, network pharmacological analyses revealed that, besides the PI3K/AKT/GSK3β signaling pathway, the NF-κB signaling pathway and the glycan AGE-RAGE signaling pathway in diabetic complications play a crucial role in the pathological process of CKD fibrosis treated with AE. Activation of RAGE promotes NADPH oxidase-mediated reactive oxygen species (ROS) generation, which thereafter triggers endoplasmic reticulum stress, glomerular hypertrophy, podocyte injury, inflammatory responses and renal fibrosis.[57] Furthermore, numerous studies have demonstrated that controlling the inflammatory response initiated by the NF-κB signaling pathway can successfully improve renal fibrosis.[28,58] These mechanisms are expected to provide new directions for studying AE in the treatment of renal fibrosis.

In summary, AE has a multifaceted therapeutic role in attenuating renal fibrosis. Meanwhile, our study suggests that the regulation of the PI3K/Akt/GSK3β pathway is central to its mechanism of action (Figure 7). Through this pathway, AE can inhibit PI3K activation in *ex vivo* models thereby hindering the PI3K/Akt/GSK3β signaling cascade and reducing the expression of fibrotic proteins such as Vimentin and α-SMA. More importantly, the above biological process is mediated by the binding of AE to specific sites of PI3K, thereby interrupting the signaling cascade and preventing the overproduction of matrix proteins. However, our study is still insufficient and the effects of AE on renal fibroblast activation and EMT, processes that are critical for the progression of renal fibrosis, should be further explored. With a more comprehensive grasp of these mechanisms, AE may indeed hold the key to innovative therapeutic strategies against CKD and renal fibrosis.

References

1. Jha V, Garcia-Garcia G, Iseki K, Li Z, Naicker S, Plattner B, et al. Chronic kidney disease: global dimension and perspectives. Lancet 2013;382:260-72.
2. Liu Y. Kidney fibrosis: fundamental questions, challenges, and perspectives. Integr Med Nephrol Androl 2024;11:e24-00027.
3. Rosa BA, Ahmed M, Singh DK, Choreno-Parra JA, Cole J, Jimenez-Alvarez LA, et al. IFN signaling and neutrophil degranulation transcriptional signatures are induced during SARS-CoV-2 infection. Commun Biol 2021;4:290.
4. Zhang YY, Tan RZ, Yu Y, Niu YY, Yu C. LncRNA GAS5 protects against TGF-beta-induced renal fibrosis via the Smad3/miRNA-142-5p axis. Am J Physiol-Renal 2021;321: F517-26.
5. Rui-Zhi T, Hui D, Jian-Chun L, Xia Z, Xiao-Jia W, Dan W, et al. Astragalus mongholicus bunge and panax notoginseng formula (A&P) combined with bifidobacterium contribute a renoprotective effect in chronic kidney disease through inhibiting macrophage inflammatory response in kidney and intestine. Front Physiol 2020;11:583668.
6. Zhu W, Chen M, Wang Y, Chen Y, Zhang Y, Wang Y, et al.

Regulation of renal lipid deposition in diabetic nephropathy on morroniside via inhibition of NF-KB/TNF-a/SREBP1c signaling pathway. Chem-Biol Interact 2023;385:110711.
7. Zhu T, Du Y, Xuan M, Guo C, Rao X. Clinical characteristics and Chinese Medicine therapy of chronic kidney disease combined with cardiovascular disease. Integr Med Nephrol Androl 2023;10:e00023.
8. Chen R, Zhang J, Hu Y, Wang S, Chen M, Wang Y. Potential antineoplastic effects of Aloe-emodin: a comprehensive review. Am J Chinese Med 2014;42:275-88.
9. Dong X, Zeng Y, Liu Y, You L, Yin X, Fu J, et al. Aloe-emodin: A review of its pharmacology, toxicity, and pharmacokinetics. Phytother Res 2020;34:270-81.
10. Lian LH, Park EJ, Piao HS, Zhao YZ, Sohn DH. Aloe emodin-induced apoptosis in t-HSC/Cl-6 cells involves a mitochondria-mediated pathway. Basic Clin Pharmacol 2005;96:495-502.
11. Friedman SL. Seminars in medicine of the Beth Israel Hospital, Boston. The cellular basis of hepatic fibrosis. Mechanisms and treatment strategies. New Engl J Med 1993;328:1828-35.
12. Woo SW, Nan JX, Lee SH, Park EJ, Zhao YZ, Sohn DH. Aloe emodin suppresses myofibroblastic differentiation of rat hepatic stellate cells in primary culture. Pharmacol Toxicol 2002;90:193-8.
13. Meng XM, Nikolic-Paterson DJ, Lan HY. TGF-beta: the master regulator of fibrosis. Nat Rev Nephrol 2016;12:325-38.
14. Yang F, Li T, Zhang XQ, Gong Y, Su H, Fan J, et al. Screening of active components in Astragalus mongholicus Bunge and Panax notoginseng formula for anti-fibrosis in CKD: nobiletin inhibits Lgals1/PI3K/AKT signaling to improve renal fibrosis. Renal Failure 2024;46:2375033.
15. He W, Dai C, Li Y, Zeng G, Monga SP, Liu Y. Wnt/beta-catenin signaling promotes renal interstitial fibrosis. J Am Soc Nephrol 2009;20:765-76.
16. Liu Y. Renal fibrosis: new insights into the pathogenesis and therapeutics. Kidney Int 2006;69:213-7.
17. Jia J, Xu LH, Deng C, Zhong X, Xie KH, Han RY, et al. Hederagenin ameliorates renal fibrosis in chronic kidney disease through blocking ISG15 regulated JAK/STAT signaling. Int Immunopharmacol 2023;118:110122.
18. Wu S, Ge Y, Lin K, Liu Q, Zhou H, Hu Q, et al. Telomerase RNA TERC and the PI3K-AKT pathway form a positive feedback loop to regulate cell proliferation independent of telomerase activity. Nucleic Acids Res 2022;50:3764-76.
19. Zhang Z, Wu W, Fang X, Lu M, Wu H, Gao C, et al. Sox9 promotes renal tubular epithelial−mesenchymal transition and extracellular matrix aggregation via the PI3K/AKT signaling pathway. Mol Med Rep 2020;22:4017-30.
20. Liu B, Deng J, Jie X, Lu F, Liu X, Zhang D. Protective effects of the Bupi Yishen formula on renal fibrosis through PI3K/AKT signaling inhibition. J Ethnopharmacol 2022;293: 115242.
21. Sharma M, Chuang WW, Sun Z. Phosphatidylinositol 3-kinase/Akt stimulates androgen pathway through GSK3beta inhibition and nuclear beta-catenin accumulation. J Biol Chem 2002;277:30935-41.
22. Singh SP, Tao S, Fields TA, Webb S, Harris RC, Rao R. Glycogen synthase kinase-3 inhibition attenuates fibroblast activation and development of fibrosis following renal ischemia-reperfusion in mice. Dis Model Mech 2015;8:931-40.
23. Bader GD, Hogue CW. An automated method for finding molecular complexes in large protein interaction networks. BMC Bioinform 2003;4:2.
24. Liu Y, Yang X, Gan J, Chen S, Xiao ZX, Cao Y. CB-Dock2: improved protein-ligand blind docking by integrating cavity detection, docking and homologous template fitting. Nucleic Acids Res 2022;50:W159-64.
25. Dou F, Liu Y, Liu L, Wang J, Sun T, Mu F, et al. Aloe-emodin ameliorates renal fibrosis via inhibiting PI3K/Akt/mTOR signaling pathway in vivo and in vitro. Rejuv Res 2019;22:218-29.
26. El-Abhar H, Abd EFM, Wadie W, El-Tanbouly DM. Cilostazol disrupts TLR-4, Akt/GSK-3beta/CREB, and IL-6/JAK-2/STAT-3/SOCS-3 crosstalk in a rat model of Huntington's disease. PLoS One 2018;13:e0203837.
27. Liu S, Chen X, Zhang S, Wang X, Du X, Chen J, et al. miR−106b−5p targeting SIX1 inhibits TGF−beta1−induced pulmonary fibrosis and epithelial−mesenchymal transition in asthma through regulation of E2F1. Int J Mol Med 2021;47:04855.
28. Wang Y, Liu P, Ma G, Wu C, Zhu W, Sun P, et al. Mechanism of dioscin ameliorating renal fibrosis through NF−kappaB signaling pathway−mediated inflammatory response. Mol Med Rep 2023;27:93.
29. Feng X, Chen L, Guo W, Zhang Y, Lai X, Shao L, et al. Graphene oxide induces p62/SQSTM-dependent apoptosis through the impairment of autophagic flux and lysosomal dysfunction in PC12 cells. Acta Biomater 2018;81:278-92.
30. Xi R, Pan S, Chen X, Hui B, Zhang L, Fu S, et al. HPV16 E6-E7 induces cancer stem-like cells phenotypes in esophageal squamous cell carcinoma through the activation of PI3K/Akt signaling pathway in vitro and in vivo. Oncotarget 2016;7:57050-65.
31. Tan RZ, Li JC, Liu J, Lei XY, Zhong X, Wang C, et al. BAY61-3606 protects kidney from acute ischemia/reperfusion injury through inhibiting spleen tyrosine kinase and suppressing inflammatory macrophage response. Faseb J 2020;34: 15029-46.
32. Xiao J, Meng XM, Huang XR, Chung AC, Feng YL, Hui DS, et al. miR-29 inhibits bleomycin-induced pulmonary fibrosis in mice. Mol Ther 2012;20:1251-60.
33. Qu H, Liu L, Liu Z, Qin H, Liao Z, Xia P, et al. Blocking TBK1 alleviated radiation-induced pulmonary fibrosis and epithelial-mesenchymal transition through Akt-Erk inactivation. Exp Mol Med 2019;51:1-17.
34. Ma Y, Wang M, Li N, Wu R, Wang X. Bleomycin-induced nuclear factor-kappaB activation in human bronchial epithelial cells involves the phosphorylation of glycogen synthase kinase 3beta. Toxicol Lett 2009;187:194-200.
35. Hill NR, Fatoba ST, Oke JL, Hirst JA, O'Callaghan CA, Lasserson DS, et al. Global prevalence of chronic kidney disease - A systematic review and meta-analysis. PLoS One 2016;11:e0158765.
36. Mu L, Zhu L, Feng Y, Chen N, Wang F, He L, et al. Nephropathy 1st inhibits renal fibrosis by activating the PPARgamma signaling pathway. Front Pharmacol 2022;13:992421.
37. Walther CP, Winkelmayer WC, Richardson PA, Virani SS, Navaneethan SD. Renin-angiotensin system blocker discontinuation and adverse outcomes in chronic kidney disease. Nephrol Dial Transpl 2021;36:1893-9.
38. Ni YH, Deng HF, Zhou L, Huang CS, Wang NN, Yue LX, et al. Ginsenoside Rb1 ameliorated bavachin-induced renal fibrosis via suppressing Bip/eIF2alpha/CHOP signaling-mediated EMT. Front Pharmacol 2022;13:872474.
39. Xiao D, Zhang Y, Wang R, Fu Y, Zhou T, Diao H, et al. Emodin alleviates cardiac fibrosis by suppressing activation of cardiac fibroblasts via upregulating metastasis associated protein 3.

Acta Pharm Sin B 2019;9:724-33.
40. Zhang Y, Song Z, Huang S, Zhu L, Liu T, Shu H, et al. Aloe emodin relieves Ang II-induced endothelial junction dysfunction via promoting ubiquitination mediated NLRP3 inflammasome inactivation. J Leukocyte Biol 2020;108:1735-46.
41. Liang Y, Jing Z, Deng H, Li Z, Zhuang Z, Wang S, et al. Soluble epoxide hydrolase inhibition ameliorates proteinuria-induced epithelial-mesenchymal transition by regulating the PI3K-Akt-GSK-3beta signaling pathway. Biochem Bioph Res Co 2015;463:70-5.
42. Cheng Y, Zhang J, Guo W, Li F, Sun W, Chen J, et al. Up-regulation of Nrf2 is involved in FGF21-mediated fenofibrate protection against type 1 diabetic nephropathy. Free Radical Bio Med 2016;93:94-109.
43. Eddy AA. Molecular basis of renal fibrosis. Pediatr Nephrol 2000;15:290-301.
44. Cai FF, Bian YQ, Wu R, Sun Y, Chen XL, Yang MD, et al. Yinchenhao decoction suppresses rat liver fibrosis involved in an apoptosis regulation mechanism based on network pharmacology and transcriptomic analysis. Biomed Pharmacother 2019;114:108863.
45. Wei S, Wang Q, Zhou H, Qiu J, Li C, Shi C, et al. miR-455-3p alleviates hepatic stellate cell activation and liver fibrosis by suppressing HSF1 expression. Mol Ther-Nucl Acids 2019;16:758-69.
46. Zhou T, Luo M, Cai W, Zhou S, Feng D, Xu C, et al. Runt-related transcription factor 1 (RUNX1) promotes TGF-beta-induced renal tubular epithelial-to-mesenchymal transition (EMT) and renal fibrosis through the PI3K subunit p110delta. eBioMedicine 2018;31:217-25.
47. Peng M, Zheng Z, Chen S, Fang L, Feng R, Zhang L, et al. Sensitization of non-small cell lung cancer cells to gefitinib and reversal of epithelial-mesenchymal transition by aloe-emodin via PI3K/Akt/TWIS1 signal blockage. Front Oncol 2022;12:908031.
48. Ma JW, Hung CM, Lin YC, Ho CT, Kao JY, Way TD. Aloe-emodin inhibits HER-2 expression through the downregulation of Y-box binding protein-1 in HER-2-overexpressing human breast cancer cells. Oncotarget 2016;7:58915-30.
49. Zhu X, Li Q, Hu G, Wang J, Hu Q, Liu Z, et al. BMS−345541 inhibits airway inflammation and epithelial−mesenchymal transition in airway remodeling of asthmatic mice. Int J Mol Med 2018;42:1998-2008.
50. Wang J, Hu K, Cai X, Yang B, He Q, Wang J, et al. Targeting PI3K/AKT signaling for treatment of idiopathic pulmonary fibrosis. Acta Pharm Sin B 2022;12:18-32.
51. Qin W, Cao L, Massey IY. Role of PI3K/Akt signaling pathway in cardiac fibrosis. Mol Cell Biochem 2021;476:4045-59.
52. Liu B, Lin J, Bai L, Zhou Y, Lu R, Zhang P, et al. Paeoniflorin inhibits mesangial cell proliferation and inflammatory response in rats with mesangial proliferative glomerulonephritis through PI3K/AKT/GSK-3beta pathway. Front Pharmacol 2019;10:978.
53. Hong H, Chen F, Qiao Y, Yan Y, Zhang R, Zhu Z, et al. GSK-3beta activation index is a potential indicator for recurrent inflammation of chronic rhinosinusitis without nasal polyps. J Cell Mol Med 2017;21:3633-40.
54. Hung PH, Hsu YC, Chen TH, Ho C, Lin CL. The histone demethylase inhibitor GSK-J4 is a therapeutic target for the kidney fibrosis of diabetic kidney disease via DKK1 modulation. Int J Mol Sci 2022;23:9407.
55. Ren J, Wei H, Sun J, Feng X, Zhang Y, Yuan H, et al. GSK3beta-dependent lysosome biogenesis: An effective pathway to mitigate renal fibrosis with LM49. Front Pharmacol 2022;13:925489.
56. Zhao JH. Mesangial cells and renal fibrosis. Adv Exp Med Biol 2019;1165:165-94.
57. Pathomthongtaweechai N, Chutipongtanate S. AGE/RAGE signaling-mediated endoplasmic reticulum stress and future prospects in non-coding RNA therapeutics for diabetic nephropathy. Biomed Pharmacother 2020;131:110655.
58. Liao Y, Tan RZ, Li JC, Liu TT, Zhong X, Yan Y, et al. Isoliquiritigenin attenuates UUO-induced renal inflammation and fibrosis by inhibiting Mincle/Syk/NF-kappa B signaling pathway. Drug Des Devel Ther 2020;14:1455-68.

Received: 7 May 2024. Accepted: 30 June 2025.

European Journal of Histochemistry 2025; 69:4228
doi:10.4081/ejh.2025.4228

Introduction

Chronic kidney disease (CKD) impacts approximately 10% of people worldwide, presenting a growing health concern. The defining characteristic of this condition is the irreversible deterioration of kidney function over time, which ultimately progresses to uremia.[1] Kidney fibrosis is a common consequence of progressive renal diseases.[2] The process involves extracellular matrix (ECM) deposition, cellular scarring, and kidney structure destruction, eventually leading to end-stage kidney disease.[3] Although there has been further understanding of the pathophysiology of CKD in recent years, current treatment strategies are still limited to slowing the disease's progression rather than reversing established kidney fibrosis.[4] Chinese Herbal Medicine (CHM), after decades of extensive research, has shown that some medicinal herbs, especially their extracted compounds, can treat various diseases and gradually elucidate their potential mechanisms.[5,6] Therefore, CHM may offer a novel and effective solution for managing CKD fibrosis.[7]

Aloe-emodin (AE) is an isomer of emodin, an anthraquinone derivative commonly found in aloe and rhubarb. It has garnered attention due to its wide range of biological activities, including immunomodulatory, anti-viral, anti-inflammatory, neuroprotective, anti-cancer and hepatoprotective properties.[8] It shows remarkable potential in treating various diseases such as inflammatory diseases, growth disorders, sepsis, malaria, liver fibrosis, flu, type 2 diabetes and psoriasis.[9] Notably, AE can inhibit the proliferation of transformed rat hepatic stellate cells by activating Caspase-9 in the mitochondrial pathway to induce apoptosis;[10] it can also significantly suppress the production of type I collagen and the expression α-smooth muscle actin (α-SMA) in hepatic stellate cells.[11,12] Current research has revealed AE's capability to combat fibrosis, offering new insights into therapeutic approaches for kidney fibrosis. Multiple mechanisms of kidney fibrosis have been confirmed. These include the TGF-β/Smad,[13] PI3K/Akt[14], Wnt/β-Catenin,[15] MAPK/ERK,[16] and JAK/STAT[17]signaling pathways. Among them, the PI3K/Akt signaling pathway is one of the key intracellular signaling pathways that modulate a variety of cellular processes such as proliferation, survival, growth, and metabolism.[18] This pathway has a strong impact on the pathophysiological process of excessive deposition of ECM proteins[19] - one of the hallmark features of fibrotic kidney disease. Liu *et al.* discovered that the Bupi Yishen formula inhibits the activity of PI3K/AKT signaling induced by adenine in rat kidneys and reduces the activation of PI3K/AKT signaling in TGF-β1-induced human proximal renal tubular cells (HK-2) in a dose-dependent manner, thereby alleviating kidney fibrosis.[20] Meanwhile, Glycogen synthase kinase 3 beta (GSK3β) is an important downstream target in the PI3K/Akt signaling pathway and participates in various biological mechanisms.[21] Research has found that inhibiting GSK3β can reduce fibrosis in AKI mice.[22] The results of these studies indicate that GSK3β plays a role in the pathogenesis of renal fibrosis following injury. Furthermore, inhibition of GSK3β prevented the progression of fibrosis even after injury had occurred, highlighting its importance as a therapeutic target. Based on the above analysis, we can hypothesize that modulating the activity of the PI3K/Akt/GSK3β signaling axis can help control or reverse the progression of kidney fibrosis caused by other chronic kidney diseases. Therefore, our study proposed to delve into the protective effects of AE on CKD-induced renal fibrosis, focusing on its effects on the PI3K/Akt/GSK-3β signaling axis. We used adenine-induced C57BL/6 mice and TGF-β1-induced HK-2 cells to investigate the effects of AE on CKD fibrosis. Additionally, we investigated the molecular mechanisms of AE in CKD fibrosis and the role of the PI3K/Akt/GSK3β signaling pathway using network pharmacology. This study aims to verify that AE improves renal fibrosis by inhibiting the PI3K/Akt/GSK3β pathway.

Materials and Methods

Prediction of targets

The targets of AE were acquired from the Traditional Chinese Medicine System Pharmacology Database (TCMSP, https://old.tcmsp-e.com/tcmsp.php). The protein name was also normalized through the UniProtKB database (http://www.uniprot.org) with the species restriction "Homo sapiens". GeneCards (http://www.genecards.org) provided Disease-related targets. The search keywords were "Chronic kidney disease" and "Kidney fibrosis", the category was "protein" and the species filter was "*Homo sapiens*".

Construction of protein-protein interaction (PPI) network and biological analysis. The corresponding targets of AE, CKD, and kidney fibrosis were plotted on the Venn to obtain the intersecting targets. Subsequently, we imported the potentially interacting targets into the String database (http://string-db.org/) and constructed a PPI network with the parameters "*Homo sapiens*", a minimum interaction score of 0.400, hiding unconnected points, and the rest of the parameters by default. Cytoscape software will be used to further analyze the PPI network, and the MCODE[23] plug-in will be used to perform the computational analysis of the nodes in the PPI network to filter out a subset of the most important ones (Degree Cutoff: 2; Node Score Cutoff: 0.2; K-Core: 2; Max Depth: 100).

To investigate the biological functions and biological pathways of the intersecting targets, Gene Ontology (GO) enrichment analysis was conducted using the Metascape database (http://www.metascape.org/) and Kyoto Encyclopedia of Genes and Genomes (KEGG) pathway analysis. The results were presented through the CNSknowall platform (https://cnsknowall.com). A p-value <0.05 was accepted.

Molecular docking

The PI3K protein crystal structure (PDB ID: 5DXT) was sourced from the RCSB PDB database (https://www.rcsb.org/) and the small molecule 3D structure was sourced from the PubChem database (https://pubchem.ncbi.nlm.nih.gov/). Docking was achieved through the utilization of blind docking on the CB-DOCK2 online server (https://cadd.labshare.cn/cb-dock2/php/blinddock.php).[24] The CB-DOCK2 system employs artificial neural networks for cavity probing and utilizes the Autodock Vina docking algorithm. All parameters of CB-DOCK2 are set to default, such as number of cavities for docking: 5. The results of the docking procedure will be selected based on the binding energy. Subsequent kinetic verification of binding stability will be conducted through force analysis and docking position assessment. Ligand-receptor force analysis was conducted with the aid of the PLIP online server (https://plip-tool.biotec.tu-dresden.de/plip-web), while the ligand-receptor 3D conformation was visualised using Pymol software.

In vivo study

Fifty 8-week-old male C57BL/6 mice (Viewsolid Biotechnologies, Beijing, China) were housed in specific pathogen-free (SPF) surroundings with 25°C temperature, 65% relative humidity and a 12 h light/dark cycle, and were allowed to access water and food *ad libitum*. After compliant feeding, the mice were randomly divided equally into five groups as follows: Control, Control+AE (20 mg/kg/day), adenine (50 mg/kg/day), AE10 (10 mg/kg/day), AE20 (20 mg/kg/day).[25] AE10 and AE20 were both administered in adenine were administered based on adenine. Adenine and AE were dissolved in purified water and 0.5% sodium carboxymethyl cellulose, respectively. Interventions

were carried out for 1 week, during which time mice were collected in urine and subsequently euthanized humanely, followed by blood and tissue samples.

Histopathology and immunohistochemistry

Kidney tissue specimens were fixed in 4% paraformaldehyde (Servicebio, Wuhan, China) overnight at 4°C, then dehydrated, cleared, and embedded in paraffin. Consecutive sections (2-5 μm thick) were cut.[26] For histology, sections underwent standard hematoxylin (G1004, Servicebio) and eosin (G1001, Servicebio) staining (H&E) and Masson's trichrome staining (G1006 kit, Servicebio) following established protocols.[27] For immunohistochemistry (IHC), deparaffinized sections underwent antigen retrieval (citrate buffer, pH 6.0, 95°C, 20 min), endogenous peroxidase blocking (3% H_2O_2, 15 min, RT), and blocking (5% BSA, 30 min, RT). Sections were incubated overnight at 4°C with primary antibodies: Fibronectin (Rabbit polyclonal, 1:1500, GB114491-100, Servicebio) and Collagen I (Rabbit polyclonal, 1:1000, GB11022-3-100, Servicebio). Negative controls used PBS instead of primary antibody. After washing, sections were incubated with HRP-conjugated Goat Anti-Rabbit IgG secondary antibody (1:200, GB23303, Servicebio) for 50 min at RT. Signal was visualized with DAB (G1211-200T, Servicebio) followed by nuclear counterstaining with Mayer's haematoxylin (G1004, Servicebio) for 1 min. Negative controls were conducted by omitting the primary antibody to ensure specificity of the staining. Slides were dehydrated, cleared, mounted, and examined under a light microscope (BX53, Olympus; Tokyo, Japan) with a 40x objective.[28] For each sample, three randomly selected fields were analyzed to ensure representative data. Image analysis was conducted using ImageJ software to quantify the percentage of positively stained cells. Three randomly selected fields per sample were analyzed, and the average percentage of immune-positive cells was reported.

Cell culture and treatment

HK-2 cells were cultured in Dulbecco's Modified Eagle's Medium (DMEM)/F-12 containing 10% foetal bovine serum (FBS, CellMax, Australia) and 1% penicillin/streptomycin, in an incubator at 37°C and 5% CO_2. TGF-β1 (10 ng/ml) induced HK-2 cells as an *in vitro* model of renal fibrosis. Then, the cells were treated with different levels of AE (CAS: 418-72-1, purity >98.0%, cat: SA8200, Solarbio Science & Technology, Beijing, China) and 740Y-P (30 μM, MCE, Monmouth Junction, NJ, USA) for 24 h.[29]

Cell proliferation assay

The effect of AE on TGF-β1-induced proliferation of HK-2 cells was assessed utilizing the Cell Counting Kit-8 (CCK-8) according to the instructions. 1×10^5 HK-2 cells were inoculated into each well of a 96-well plate and waited until the cells were attached to the wall, then different concentrations of AE were added to treat the TGF-β1-induced cells. After this, add 10 μL of CCK-8 solution and keep for 1 h. Cell proliferation was analyzed according to the results measured by the zymography (450 nm). Furthermore, the results were replicated 8 times for each concentration.

Plasmid and siRNA transfection of cells

The coding sequence of PIK3CA was cloned into the pcDNA3.1 vector (Beyotime, Shanghai, China). The structure of the specific locus was changed using a rapid mutation system. Transfect the plasmid using the liposomal lip3000 method. Ensure that the cells are 70-80% covered in the 6-well plate before the experiment. Heat the DMEM water bath at 37°C and place the transfection reagents and DNA plasmid at room temperature. Prepare two centrifuge tubes, add 125 μL DMEM to each tube, add lipofectamine 3000 μL to tube 1, and incubate at room temperature for 5 min; 2.5 μg DNA plasmid was added to tube 2 and the two centrifuge tubes were mixed and left to stand at room temperature for 5 min. When the DNA liposomes were left to stand for 4 min, HK-2 cells to be transfected were taken out from the 37°C incubator, and the DNA liposomes were incubated with DMEM. C incubator, gently over-washed with DMEM and then added DMEM 1.5 mL/well. When the time was up, 0.25 mL of DNA-liposome mixture was added drop by drop into the culture dish, and the dish was incubated in the incubator at 37°C with 5% CO_2 for 4-6 h, then changed to 10% FBS-DMEM culture medium, and continued to incubate for 48 h to establish a stable cell line. PI3K (siRNA) was transfected into cells *via* Liposome 3000 (Mei5 Biotechnology; Beijing, China). The target sequences[30] were sense 5′-GCUAUCCUCUGAACAACUATTdTdT-3′ and antisense 5′-UAGUUGUUCAGA GGAUAGCTTdTdT-3′.

Immunofluorescence

Pre-treated tissues and cells were incubated overnight at 4°C with primary antibodies, anti-P-Pi3k (1:100,17366S, Cell Signaling Technology, Danvers, MA, USA), anti-Pi3k (1:100, ab278545, Abcam, Cambridge, MA, USA), anti-Akt (1:200, 4691S, Cell Signaling Technology), anti-P-Akt (1:400, 4060S, Cell Signaling Technology), anti-GSK3β (1:200, K000041M, Solarbio) and anti-P-GSK3β (1:100, GB114582-100, Servicebio). The fluorescent secondary antibodies (1:800GB25301/GB28301, Servicebio) were added to the samples in a light-avoiding environment and incubated for 2 h at room temperature in the absence of light. Finally, DAPI (10 μg/mL) was incubated away from light for 5 min. Negative controls were conducted by omitting the primary antibody to ensure specificity of the staining. Immunofluorescence results were acquired through the use of laser confocal microscopy (LSM800, Zeiss, Oberkochen, Germany) in a 40x objective. Image analysis was performed using ImageJ software (National Institutes of Health). The precise methodology employed for immunofluorescence was consistent with that previously described.[31] All experiments were repeated three times.

Western blotting assay

This experiment was performed using α-SMA (1:1000, 19245S, Cell Signaling Technology), Vimentin (1:1000, ab92547, Abcam), PI3k (1:100, sc-365290, Biotechnology, Santa Cruz, CA, USA), P-Pi3k (1:1000, ab278545, Abcam), GSK3β (1:1000, K000041M, Solarbio, Beijing, China), P-GSK3β (1:300, GB114582-100, Servicebio), Akt (1:1000, 4691S, Cell Signaling Technology), P-Akt (1:1000, 4060S, Cell Signaling Technology) and β-actin (1:10,000, sc-47778, Santa Cruz Biotechnology) antibodies. Specific signals were detected using a gel imaging system program (iBright CL1000, Thermo Fisher Scientific, Waltham, MA, USA), and the above signals were analyzed using Image J software. Specific steps were performed according to the previously described.[32]

Statistical analysis

All data are expressed as mean ± SEM values. To analyze the data, multiple comparisons were performed using ANOVA (one-way analysis of variance) and Dunnett's *t*-test. A *p*-value of less than 0.05 was deemed to be statistically significant. The data were evaluated with the use of GraphPad Prism version 8.0 (GraphPad Prism Software, La Jolla, CA, USA).

Results

Acquisition of target points and construction of the PPI network

We obtained 23 biomolecular targets of AE and explored the chemical structure of AE in depth with the help of the PubChem database and KingDraw, obtaining Figure 1A. For CKD and renal fibrosis biomolecular targets, we obtained 12,850 and 7,975 respectively. By comparing the data of related proteins in three groups, we identified 21 common proteins (Figure 1B). With the help of the STRING database, we created a PPI network of the intersection proteins (Figure 1C). This network comprises 21 nodes, 75 edges, an average node degree of 7.14, and a local clustering coefficient of 0.676. The MCOD analysis of the PPI network conducted with Cytoscape software revealed the most core clustered sub-network, including CASP3, TP53, PTGS2, HSP90AB1, PIK3CA, IL1B, PRKCD, CDC42, TNF, MYC, and BAX, as shown in Figure 1D.

Enrichment analysis

To gain insight into the potential biological processes that AE may induce in renal fibrosis, the identified common genes were further analyzed. The GO analysis unveiled three main categories: biological processes (BP), cellular components (CC), and molecular functions (MF). Major biological processes include positive regulation of lipid catabolic process, programmed necrotic cell death, and positive regulation of an acute inflammatory response. Principal molecular functions identified were cytokine receptor binding, kinase regulator activity, protein kinase regulator activity, protease binding, and protein serine kinase activity. The primary cellular components involved were the nuclear periphery, neuronal cell body, cell body, transferase complex, *etc*. (Figure 1E). In furthermore, the top twenty pathways shown in Figure 1F were confirmed by KEGG enrichment analysis. It was found that eight signaling pathways, including the AGE-RAGE signaling pathway in diabetic complications, IL-17 signaling pathway, NF-kappa B signaling pathway, PI3K-Akt signaling pathway, VEGF signaling pathway, chemokine signaling pathway, hepatitis B, and human

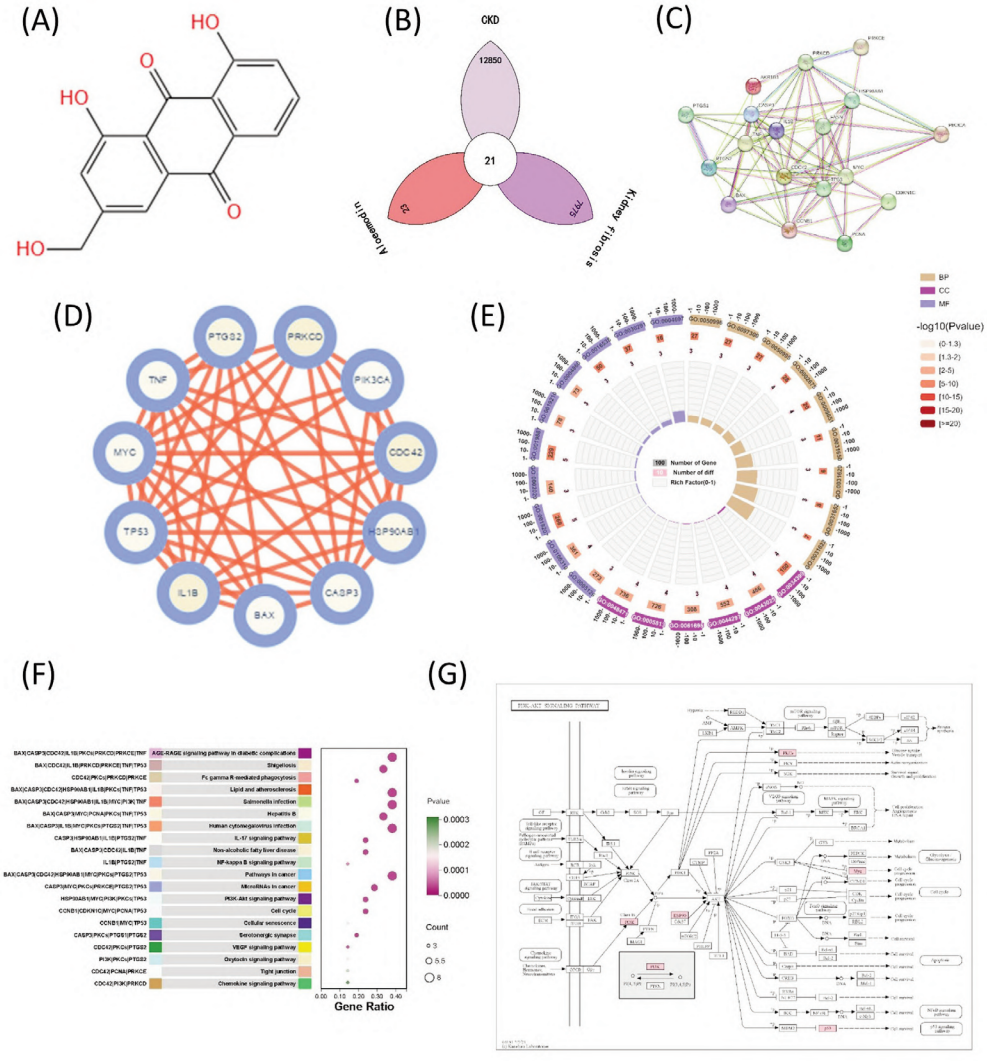

Figure 1. Network pharmacological analysis of aloe-emodin-associated proteins in CKD fibrosis. **A**) Structure of aloe-emodin. **B**) Venn diagram of overlapping proteins between CKD, kidney fibrosis and aloe-emodin related target genes. **C**) PPI network of overlapping target genes. **D**) PPI network key subset. **E**) GO enrichment analysis of predicted targets of overlapping proteins. **F**) KEGG analysis of predicted proteins of overlapping proteins. **G**) KEGG Diagram hsa04151.

cytomegalovirus infection, play key roles either directly or indirectly in the occurrence and development of inflammation and fibrosis. Therefore, it is highly likely that AE can improve the progression of renal fibrosis through the aforementioned pathways.

By utilizing the KEGG database to identify and screen the obtained signaling pathways, we discovered the PI3K-Akt signaling pathway that controls various biological reactions within cells (Figure 1G). GSK3β is identified as one of its key downstream molecules. It has been reported that multiple AKT pathways are activated in lung fibrosis models,[33] including the activation of the AKT/GSK3β signaling pathway in bronchial epithelial cells induced by bleomycin.[34] Based on these analyses, we selected the PI3K/Akt/GSK3β signaling pathway to verify the preventive and therapeutic effects of AE on kidney fibrosis.

AE alleviates renal function, renal pathologic changes and renal fibrosis in adenine-induced mice

To evaluate the effect of AE on adenine-induced kidney injury in mice, we conducted oral administration of drugs to the mice for one week. The findings of the experimental study demonstrated that, in comparison to the adenine model group, the AE treatment

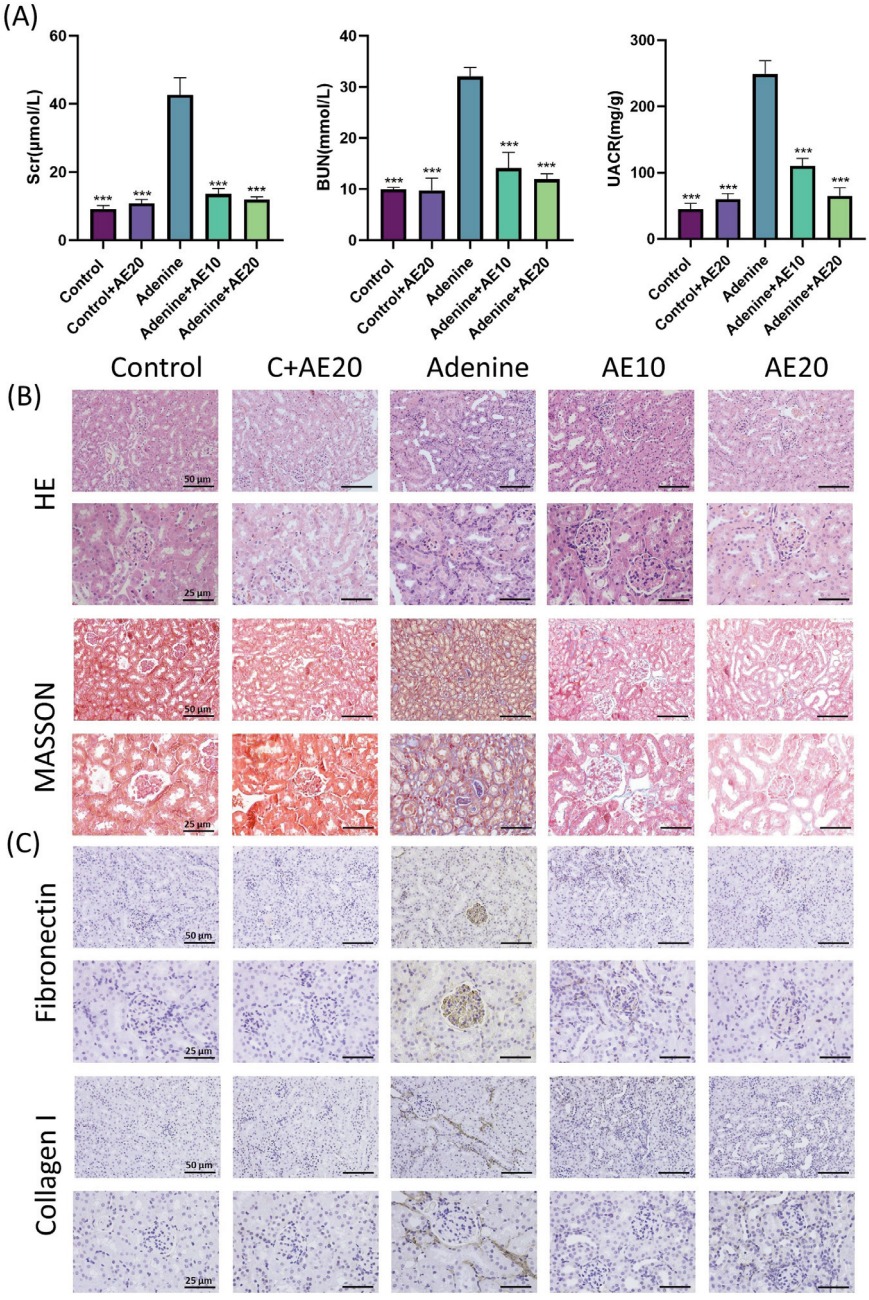

Figure 2. The effect of AE in adenine-induced mice. **A**) MOR improve the level of Scr and BUN in blood; decreased the level of UACR in urine. **B**) H&E staining reflects the extent of kidney damage in mice after 7 days of AE treatment; Masson's trichrome staining shows the extent of collagen fibril deposition in mice after 7 days of AE treatment. **C**) Immunohistochemical staining showed expression of fibronectin and collagen I after 7 days of AE treatment. Data are expressed as mean ± SD. n=10, *p<0.05; **p<0.01, ***p<0.001 compared with the model group.

regimen resulted in a notable reduction in serum creatinine (Scr), blood urea nitrogen (BUN) levels, and urine albumin/creatinine ratio (UACR), but there was no statistical difference between the high and low dose groups (Figure 2A). In Figure 2B, H&E staining showed glomerular swelling in the model group, and inflammatory cell infiltration in the kidney interstitial area; collagen fiber deposition was evident in kidney tissue sections stained with Masson's trichrome. By comparison, the kidney tissue pathology of the AE group was good. In addition, we performed IHC on the kidneys of the mice. The experiments showed that fibronectin and collagen I were widely deposited in the ECM of adenine mouse kidneys, and the addition of AE reversed the situation of kidney fibrosis (Figure 2C). Further analysis has shown that AE can be effective in decreasing the degree of glomerulosclerosis and interstitial fibrosis, and has a significant alleviating effect on adenine-induced kidney function damage and pathological changes in the kidney.

AE interferes with the PI3K/AKT/GSK3β signaling pathway in adenine-induced mice and ameliorates renal fibrosis

Network pharmacology revealed the potential mechanism of AE's effect on the kidney. We noted through immunofluorescence

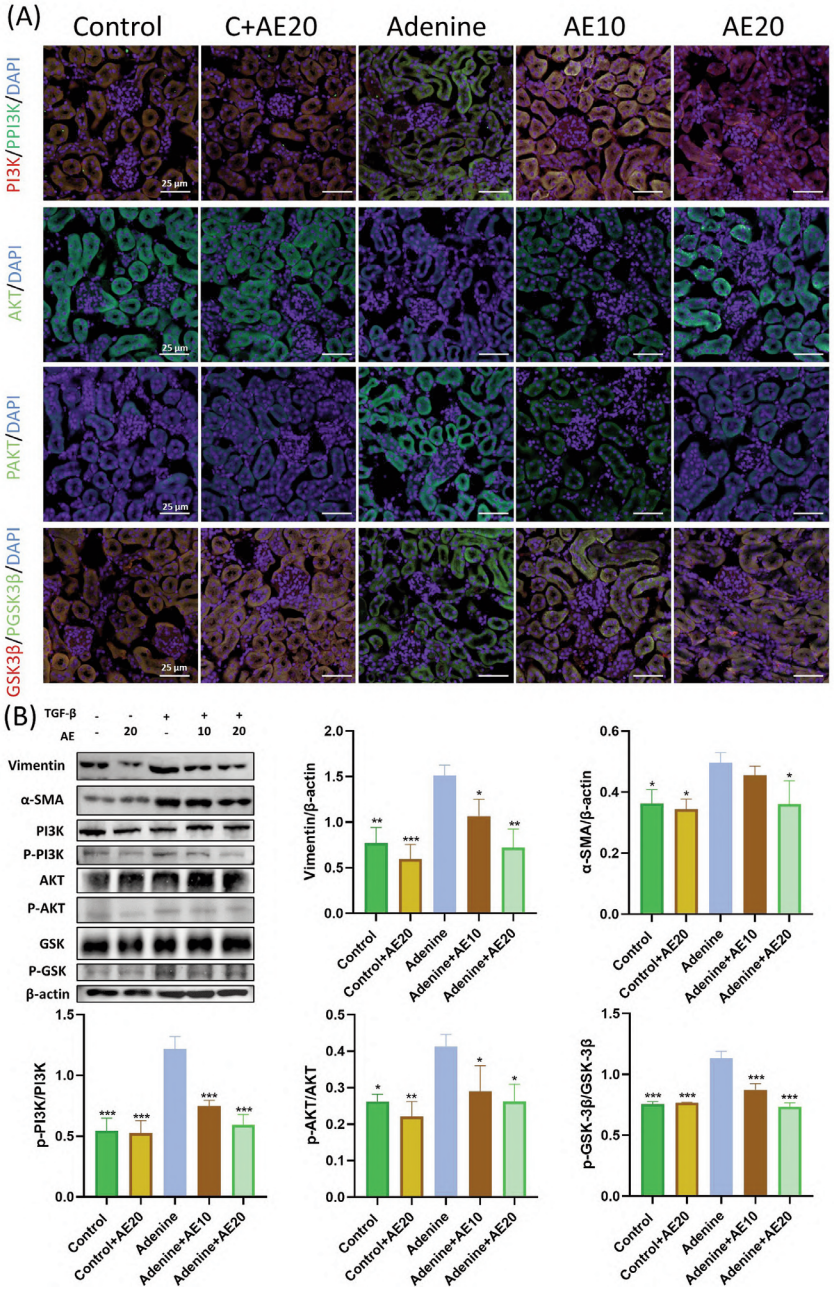

Figure 3. Regulation of PI3K/AKT/GSK3β pathway by AE in adenine-induced mice. **A**) Immunofluorescence staining of p-PI3K, PI3K, p-Akt, Akt, p-GSK3β and GSK3β in Adenine-induced mice after 7 days of AE treatment. **B**) Protein expression levels of p-PI3K/PI3K, p-Akt/Akt, p-GSK3β/GSK3β, Vimentin and α-SMA in each specific group of mice after 7 days of AE treatment. *p<0.05; **p<0.01, ***p<0.001 compared to the KKAy group.

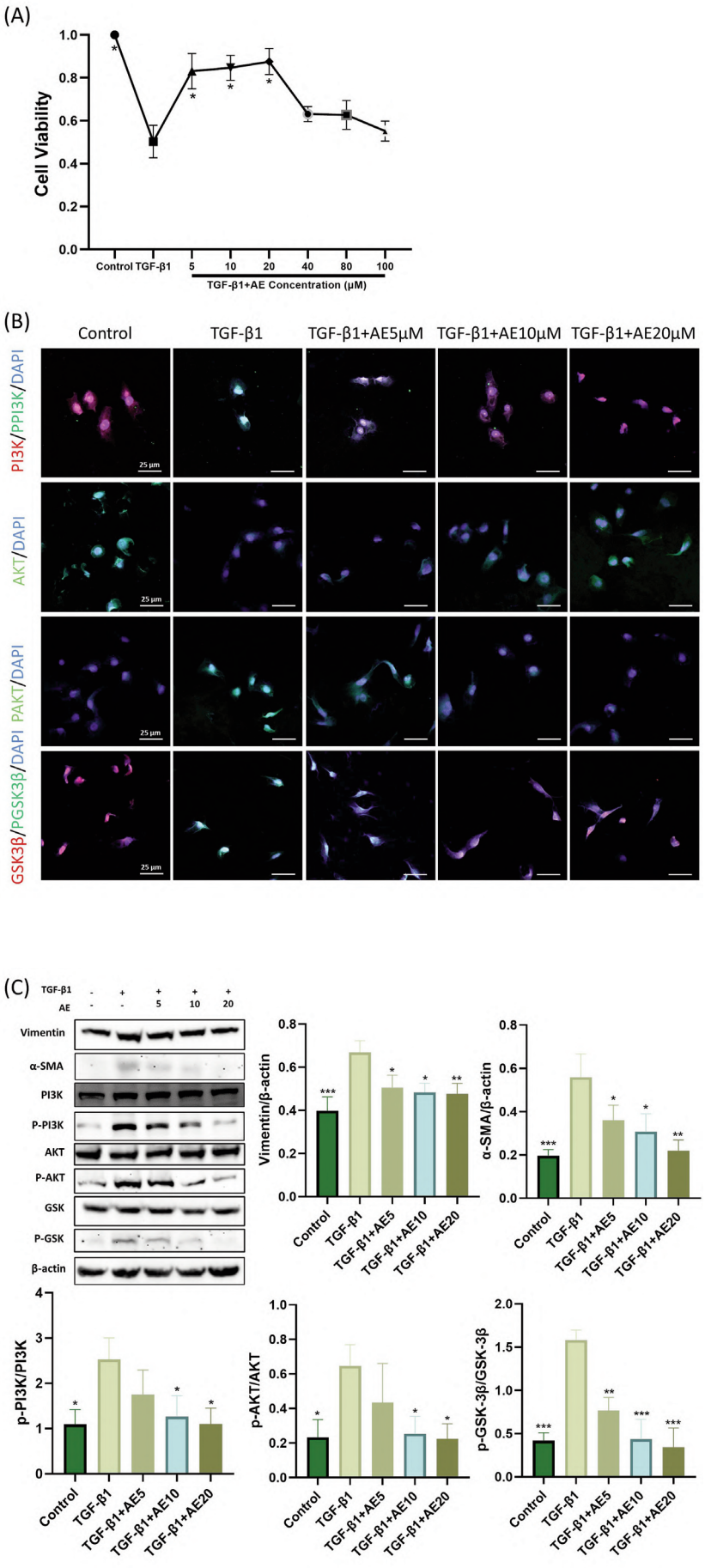

Figure 4. AE improving renal fibrosis by inhibiting the PI3K/AKT/GSK3β signaling pathway in TGFβ-1-stimulated HK-2 cells. **A**) The effect of AE on the proliferation of HK-2 cells. **B**) Immunofluorescence staining of p-PI3K, PI3K, p-Akt, Akt, p-GSK3β and GSK3β for each specific group. C) Protein expression levels of p-PI3K/PI3K, p-Akt/Akt, p-GSK3β/GSK3β, vimentin and α-SMA in each specific group of HK-2 cells. *p<0.05; **p<0.01, ***p<0.001 compared to TGFβ-1 group.

staining that the expression of phosphorylated PI3K, AKT, and GSK3β increased significantly in the kidney tissues of adenine mice. However, in the AE group, their expression levels were significantly reduced, close to the level of the control group (Figure 3A). Fortunately, our protein immunoblotting results were in line with this observation, showing significant increases in the ratios of p-PI3K/PI3K, p-Akt/Akt, and p-GSK3β/GSK3β (Figure 3B). Notably, the protein levels of the fibrotic molecules vimentin and α-SMA were also significantly increased in the adenine group and dramatically reduced after AE treatment. However, increasing the dose of AE did not seem to significantly improve its therapeutic effect, with no statistical significance. The above results imply that AE may improve kidney fibrosis by inhibiting the activation of the PI3K/AKT/GSK3β signaling pathway, which is likely related to the regulation of epithelial-mesenchymal transition.

AE inhibits PI3K/AKT/GSK3β signaling pathway activation and ameliorates TGF-β1-induced fibrosis in HK-2 cells

In order to clarify the potential mechanism of AE, we chose cell models for *in vitro* experiments to verify its anti-fibrotic effect. The results in Figure 4A show that compared to the TGF-β1 group,

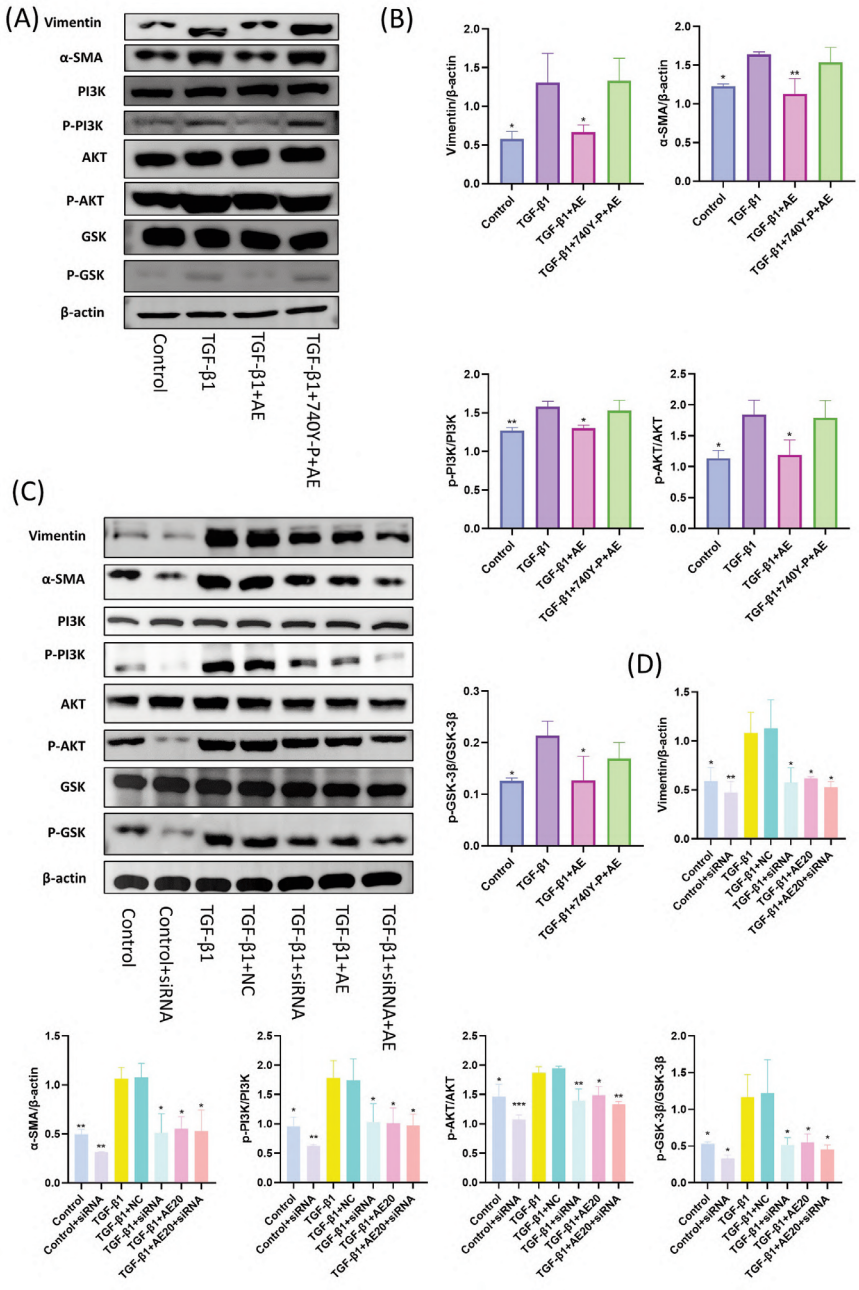

Figure 5. Inhibition and activation of PI3K alters fibrosis in HK-2 cells. **A**) Protein levels of p-PI3K, PI3K, p-Akt, Akt, p-GSK3β, GSK3β, vimentin and α-SMA in HK-2 cells in each group after 740Y-P treatment. **B**) Protein expression levels of p-PI3K/PI3K, p-Akt/Akt, p-GSK3β/GSK3β, Vimentin and α-SMA in each specific group of HK-2 cells. **C**) Protein levels of PI3K, p-Akt, Akt, p-GSK3β, GSK3β, vimentin and α-SMA in each group after PI3K silencing. **D**) Levels of p-PI3K/PI3K, p-Akt/Akt, p-GSK3β/GSK3β, vimentin and α-SMA. **p*<0.05; ***p*<0.01, ****p*<0.001 compared to TGFβ-1 group.

cell viability increased significantly with various doses of AE, and the intervention concentrations of 5 μM, 10 μM, and 20 μM worked the best. Therefore, these concentrations were used in subsequent experiments. First, we conducted immunofluorescence experiments. The experiment results show that changes in PI3K, AKT, and GSK3β in TGF-β1-induced HK-2 cells were consistent with those in adenine mouse kidneys (Figure 4B). In Western blot experiments, we observed the changes of vimentin and α-SMA in HK-2. The stimulation of TGF-β1 increased the expression of these proteins, intensifying the fibrosis of HK-2 cells. At the same time, PI3K was activated in HK-2. The ratio of p-PI3K/PI3K was highest in the model group, and then AKT and GSK3β were also activated (Figure 4C). All the above conditions were inhibited after AE treatment. These changes reveal that AE delays the fibrosis process of TGF-β1-induced HK-2 cells by inhibiting the activation of the PI3K/AKT/GSK3β signaling pathway.

Inhibition and activation of PI3K alters fibrosis in HK-2 cells

To further elucidate the role of AE and PI3K/AKT/GSK3β signaling pathways in HK-2 cell fibrosis, we performed more in-depth experiments. First, we used the cell-permeable PI3K activa-

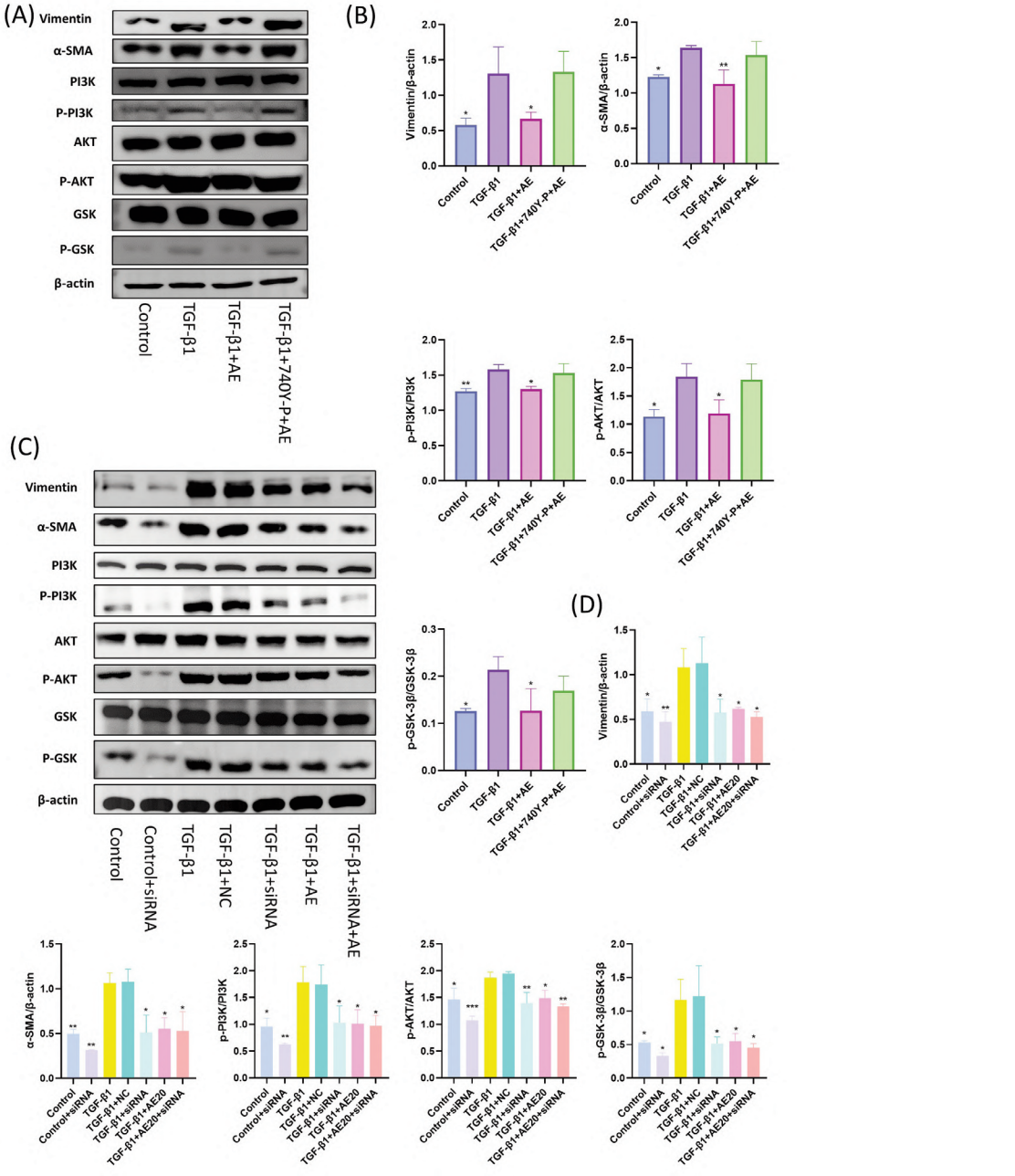

Figure 5. Inhibition and activation of PI3K alters fibrosis in HK-2 cells. **A**) Protein levels of p-PI3K, PI3K, p-Akt, Akt, p-GSK3β, GSK3β, vimentin and α-SMA in HK-2 cells in each group after 740Y-P treatment. **B**) Protein expression levels of p-PI3K/PI3K, p-Akt/Akt, p-GSK3β/GSK3β, Vimentin and α-SMA in each specific group of HK-2 cells. **C**) Protein levels of PI3K, p-Akt, Akt, p-GSK3β, GSK3β, vimentin and α-SMA in each group after PI3K silencing. **D**) Levels of p-PI3K/PI3K, p-Akt/Akt, p-GSK3β/GSK3β, vimentin and α-SMA. *p<0.05; **p<0.01, ***p<0.001 compared to TGFβ-1 group.

tor 740Y-P. As shown in Figure 5 A,B, the PI3K/AKT/GSK3β signaling pathway was fully activated and the levels of vimentin and α-SMA was significantly upregulated in the fibrosis model cells; when 740Y-P and AE stimulated fibrosis model cells simultaneously, in terms of protein expression, AE counteracted the effect of 740Y-P in activating PI3K and inhibited PI3K activation. This suggests that AE may regulate PI3K/AKT/GSK3β signaling pathway transduction and attenuate cellular fibrosis by inhibiting PI3K activation. We then transfected the siRNA of PI3K into HK-2 cells to silence its expression. In Figure 5 C,D we can see that the ratio of p-PI3K/PI3K was significantly reduced after silencing compared to the control group, as was the expression of p-Akt/Akt and p-GSK3β/GSK3β. The differences between the TGF-β1 and TGF-β1+NC groups were not statistically significant. In addition, in comparison to the model group, the TGF-β1+siRNA group demonstrated a notable reduction in the levels of Vimentin and α-SMA, which was consistent with the results of the AE group. Nevertheless, in the TGF-β1+siRNA+AE group, the superimposition of these two elements did not have a one-plus-one effect. The above results suggest that activation of PI3K promotes the progression of fibrosis, whereas inhibition of PI3K attenuates cellular fibrosis. When HK-2 cells received AE treatment, AE could slow down the fibrotic progression of the cells by inhibiting the activation of PI3K and thus modulating the PI3K/AKT/GSK3β signaling pathway.

AE exerts fibrosis inhibition by binding to specific sites of PI3K

In the present study, molecular docking experiments were conducted to confirm the mechanism of action of AE and PI3K. On docking, it was observed that a specific interaction had been formed between AE and PI3K. The binding energy between ligand and receptor was calculated to be -9.0 kcal/mol using the Vina binding energy prediction algorithm based on the AMBER force field. The protein-ligand-formed complexes were analyzed for interaction forces relying on the PLIP server and the results were subsequently presented using the molecular modelling software Pymol. In Figure 6A, we have labelled a certain number of hydrogen bonds formed by proteins with the carboxyl groups of the compounds in red and those interacting with the π-π stack in orange, and have labelled specific interacting residues in the figure with the corresponding bond lengths in angstroms next to the dashed lines. Concurrently, the analysis of the ligand-protein mutual position, when considered in conjunction with the overall analysis,

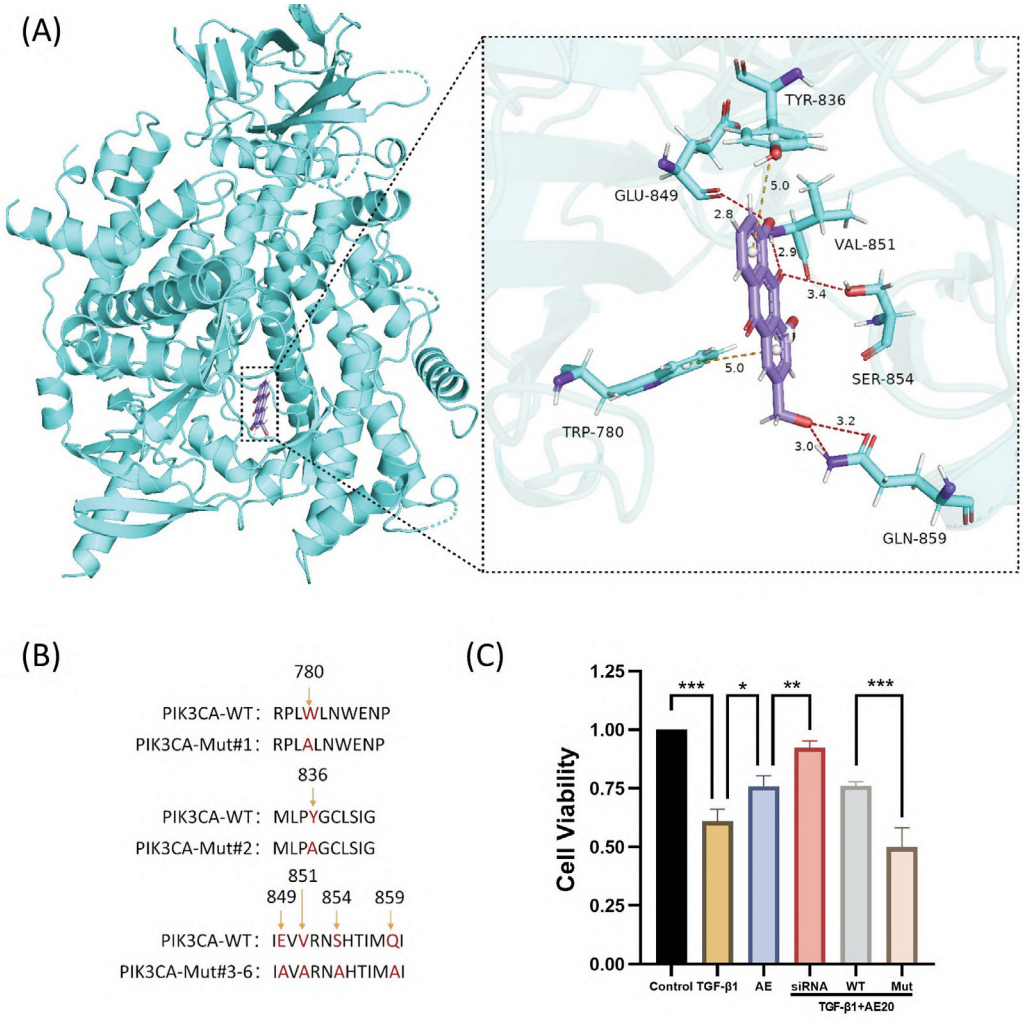

Figure 6. AE inhibits fibrosis by binding to PI3K. **A**) Predicted homology modelling structure of AE and PI3K protein binding site. **B**) Schematic diagram of PI3K mutation. **C**) PI3K-deficient HK-2 cells were re-expressed using the overexpressed plasmid, treated with AE for 24 h, and detected by CCK-8. *p<0.05; **p<0.01, ***p<0.001 compared to TGFβ-1 group.

reveals that the ligand binds to the internal cavity of the protein with low free energy, forming a specific number of hydrogen bonds and a range of interactions. It can be postulated that the ligand and the receptor form a more stable complex.

On this basis, we constructed plasmids for PI3K mutants, which included TRP-780, TYR-836, GLU849, VAL-851, SER-854 and GLN-859 (Figure 6B). To establish PI3K-deficient HK-2 cells, we overexpressed with wild-type PI3K and mutant PI3K and treated with TGF-β1 and AE, respectively. The results of the CCK-8 assay showed that wild-type PI3K significantly restored the reduced cellular activity of TGF-β1 when stimulated by AE. However, PI3K-deficient HK-2 cells caused by mutant PI3K did not increase HK-2 cell activity after TGF-β1 and AE stimulation, suggesting reduced sensitivity to AE (Figure 6C). Thus, AE can only exert its therapeutic effect by binding to specific sites of PI3K. Taken together, the results of previous experiments lead to the conclusion that AE inhibits the activity of PI3K by binding to it and ameliorates renal fibrosis by modulating the PI3K/AKT/GSK3β signaling pathway.

Discussion

CKD is a condition characterized clinically by a gradual deterioration in renal function. The underlying causes of CKD are numerous and diverse, including diabetes and hypertension.[35] The typical lesion is a gradual covering of healthy renal cells with ECM proteins, resulting in renal fibrosis.[36] However, no drugs have been approved to specifically target and directly treat renal fibrosis. Indirectly addressing renal fibrosis by controlling the progression of CKD is currently the dominant solution, including the use of standard medications such as ACE inhibitors, angiotensin II receptor blockers (ARBs) to control the causes of renal damage, and strict glycemic control in diabetic patients.[37] The identification of effective new strategies for the treatment of kidney fibrosis is therefore of great importance. The results of recent research indicate that the active ingredients of Chinese medicines may have potential antifibrotic effects,[38,39] which reveals that we may be able to discover effective anti-renal fibrosis drugs from the wealth of Chinese medicinal resources.

AE, scientifically known as 1,8-dihydroxy-3-(hydroxymethyl) anthraquinone, with a chemical molecular formula of $C_{15}H_{10}O_5$ and a relative molecular mass of 270.23, is an anthraquinone compound extracted from the roots and rhizomes of rhubarb.[40] A number of biological properties and potential therapeutic benefits have been ascribed to AE.[8] Nevertheless, the impact of AE on renal fibrosis in CKD patients remains to be determined. Using network pharmacology and basic experiments, we predicted and assessed putative AE proteins and signaling pathways against kidney fibrosis. It was revealed that AE may attenuate renal fibrosis by inhibit-

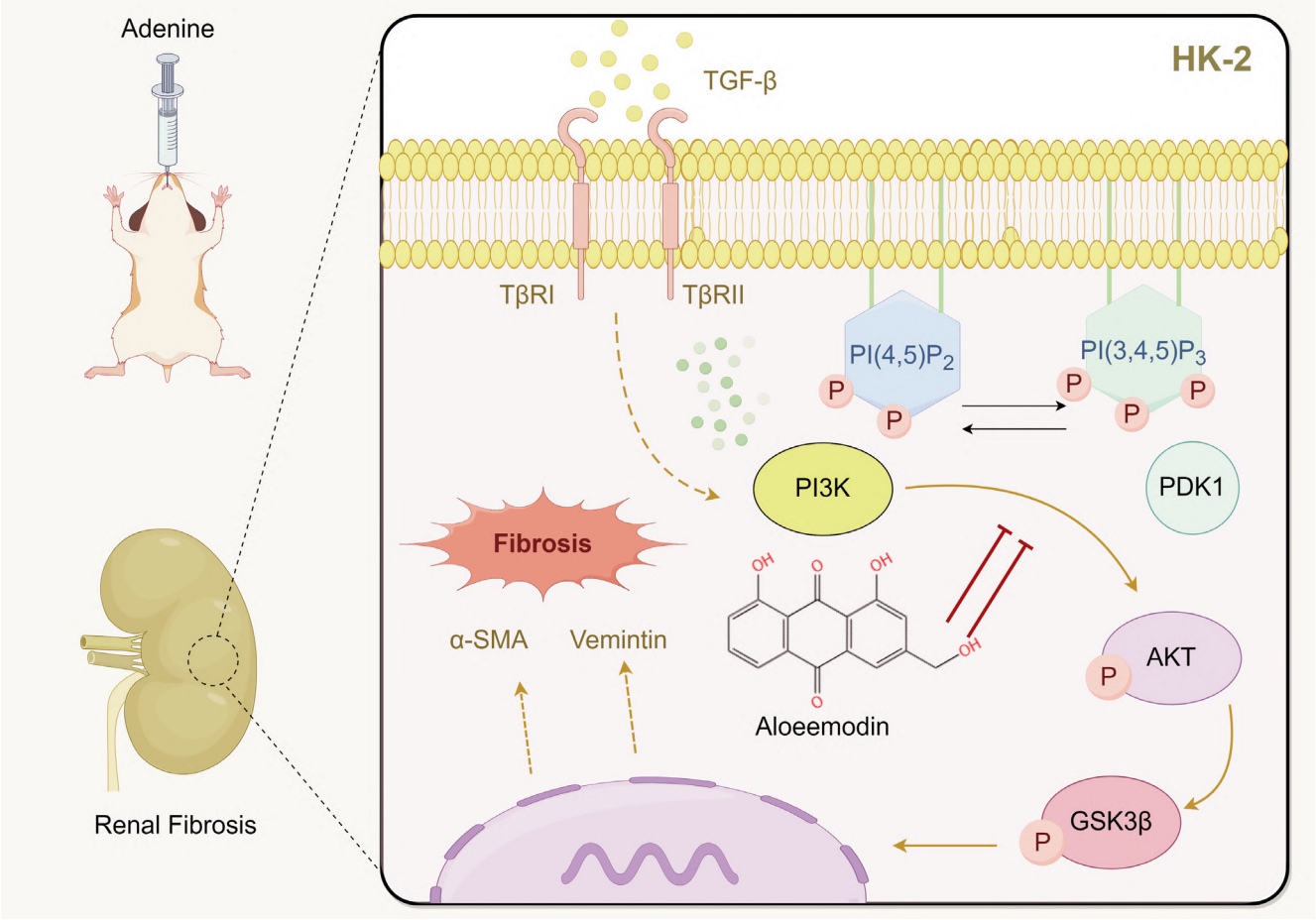

Figure 7. Schematic summary of AE amelioration of renal fibrosis through inhibition of the PI3K/AKT/GSK3β signaling pathway.

ing the PI3K/Akt/GSK3β signaling pathway (Figure 9 C-F). *In vivo* and *in vitro* analyses showed that Aloe vera rhodopsin had an inhibitory effect on kinase activity and the corresponding molecules, which is consistent with the findings of Dou *et al.*[25]. The consistency between the different models emphasizes the therapeutic role of AE through this pathway, which coincides with the study by Liang *et al.*[41] and Cheng *et al.*,[42] which provides a good basis for combating the progression of chronic renal failure.

During the experiments, we proved for the first time that AE had an antifibrotic effect and protected against renal injury using adenine-induced CKD mice. AE ameliorated histopathological abnormalities in model mice (Figure 1), reduced collagen staining area and mesangial cell proliferation, and attenuated Scr, BUN, and UACR. Also, IHC showed that AE diminished the expression of fibrotic proteins, including fibronectin and collagen I, in the kidneys of adenine mice. Fibronectin and collagen I are two key ECM proteins, and the extent to which they are deposited in the kidney is directly correlated with damage to kidney structure and function.[43] Notably, back in 2019, Cai *et al.* demonstrated that AE significantly inhibited human hepatic stellate cell proliferation and affected apoptosis,[44] and that the activation and proliferation of hepatic stellate cells played a central role in the process of liver fibrosis.[45] Recent research evidence increasingly suggests that epithelial-mesenchymal transition (EMT) is a crucial factor in the development of renal fibrosis, as transformed epithelial cells exacerbate the fibrotic process by secreting ECM proteins.[46] Meanwhile, some scholars have found that AE can inhibit and reverse EMT in a variety of cancer cells,[47,48] which makes us wonder whether AE can similarly inhibit or reverse EMT in renal tubular epithelial cells, or even reverse the process of renal fibrosis. Importantly, our study validated the capability of AE to decrease the expression of the EMT marker protein vimentin,[49] attenuate kidney injury, and inhibit renal fibrosis. Furthermore, the specific molecular mechanism of its effect was analyzed through network pharmacology and molecular docking, and the close association of AE with the PI3K/Akt/GSK3β signaling pathway was verified. The PI3K/AKT signaling pathway is of pivotal importance in the study of fibrosis, and there is an increasing recognition of its contribution to the fibrosis process. The reviews by Wang *et al.* [50] and Qin *et al.*[51] summarized and reported the findings of the PI3K/AKT pathway in idiopathic pulmonary fibrosis and cardiac fibrosis, respectively, and concluded that PI3K/AKT is a key signaling node during fibrosis, with potential significance for the development of novel antifibrotic strategies. In renal disease, a study by Liu *et al.*[52] found that Paeoniflorin was able to inhibit the proliferation and cell cycle progression of human mesenchymal cells (HMCs) and reduce the level of inflammatory factors and iNOS expression. In addition, the compound strongly inhibited the PI3K/AKT/GSK3β pathway and potentiated the effects of PI3K inhibitors, while also resisting the activating effect of insulin-like growth factor 1 (IGF-1) on this pathway. GSK3β is a key downstream signaling molecule of AKT, influencing inflammation and fibrosis.[53,54] In addition, GSK3β may represent a promising therapeutic target for renal fibrosis.[55] These findings suggest that the PI3K/AKT/GSK3β signaling pathway inhibits the activation and differentiation of HMCs and reduces the deposition of ECM, *e.g.*, collagen I, fibronectin, *etc*.,[56] thereby inhibiting fibrosis formation. The results of these analyses are in perfect agreement with our experimental performance. In the present experiments, we found that AE not only inhibited adenine-induced renal injury in mice and attenuated the expression of the fibrosis indicators vimentin and α-SMA, but also inhibited the overexpression of the PI3K/AKT/ GSK3β pathway in an *in vivo* model (Figure 3). Notably, Dou *et al.* reported similar findings, confirming that inhibition of this signaling cascade by AE plays a key role in ameliorating renal fibrosis.[25] More importantly, a series of functional analyses based on molecular docking data showed that AE failed to exert antifibrotic activity in PI3K-deficient HK-2 cells (Figure 6). As illustrated in the graph, the survival of HK-2 was decreased after TGF-β1 treatment, but cell survival was improved after AE treatment (Figure 6C). However, when the cells were treated with plasmid, the protective effect of AE on HK-2 lost its effect and cell survival decreased. The analysis of these results suggests that AE inhibits the activity of PI3K mainly by binding to PI3K, thus protecting renal function and improving fibrosis. Furthermore, the results indicate that PI3K may serve as a promising target for therapeutic intervention in the management of renal fibrosis.

Furthermore, network pharmacological analyses revealed that, besides the PI3K/AKT/GSK3β signaling pathway, the NF-κB signaling pathway and the glycan AGE-RAGE signaling pathway in diabetic complications play a crucial role in the pathological process of CKD fibrosis treated with AE. Activation of RAGE promotes NADPH oxidase-mediated reactive oxygen species (ROS) generation, which thereafter triggers endoplasmic reticulum stress, glomerular hypertrophy, podocyte injury, inflammatory responses and renal fibrosis.[57] Furthermore, numerous studies have demonstrated that controlling the inflammatory response initiated by the NF-κB signaling pathway can successfully improve renal fibrosis.[28,58] These mechanisms are expected to provide new directions for studying AE in the treatment of renal fibrosis.

In summary, AE has a multifaceted therapeutic role in attenuating renal fibrosis. Meanwhile, our study suggests that the regulation of the PI3K/Akt/GSK3β pathway is central to its mechanism of action (Figure 7). Through this pathway, AE can inhibit PI3K activation in *ex vivo* models thereby hindering the PI3K/Akt/GSK3β signaling cascade and reducing the expression of fibrotic proteins such as Vimentin and α-SMA. More importantly, the above biological process is mediated by the binding of AE to specific sites of PI3K, thereby interrupting the signaling cascade and preventing the overproduction of matrix proteins. However, our study is still insufficient and the effects of AE on renal fibroblast activation and EMT, processes that are critical for the progression of renal fibrosis, should be further explored. With a more comprehensive grasp of these mechanisms, AE may indeed hold the key to innovative therapeutic strategies against CKD and renal fibrosis.

References

1. Jha V, Garcia-Garcia G, Iseki K, Li Z, Naicker S, Plattner B, et al. Chronic kidney disease: global dimension and perspectives. Lancet 2013;382:260-72.
2. Liu Y. Kidney fibrosis: fundamental questions, challenges, and perspectives. Integr Med Nephrol Androl 2024;11:e24-00027.
3. Rosa BA, Ahmed M, Singh DK, Choreno-Parra JA, Cole J, Jimenez-Alvarez LA, et al. IFN signaling and neutrophil degranulation transcriptional signatures are induced during SARS-CoV-2 infection. Commun Biol 2021;4:290.
4. Zhang YY, Tan RZ, Yu Y, Niu YY, Yu C. LncRNA GAS5 protects against TGF-beta-induced renal fibrosis via the Smad3/miRNA-142-5p axis. Am J Physiol-Renal 2021;321: F517-26.
5. Rui-Zhi T, Hui D, Jian-Chun L, Xia Z, Xiao-Jia W, Dan W, et al. Astragalus mongholicus bunge and panax notoginseng formula (A&P) combined with bifidobacterium contribute a renoprotective effect in chronic kidney disease through inhibiting macrophage inflammatory response in kidney and intestine. Front Physiol 2020;11:583668.
6. Zhu W, Chen M, Wang Y, Chen Y, Zhang Y, Wang Y, et al.

Regulation of renal lipid deposition in diabetic nephropathy on morroniside via inhibition of NF-KB/TNF-a/SREBP1c signaling pathway. Chem-Biol Interact 2023;385:110711.
7. Zhu T, Du Y, Xuan M, Guo C, Rao X. Clinical characteristics and Chinese Medicine therapy of chronic kidney disease combined with cardiovascular disease. Integr Med Nephrol Androl 2023;10:e00023.
8. Chen R, Zhang J, Hu Y, Wang S, Chen M, Wang Y. Potential antineoplastic effects of Aloe-emodin: a comprehensive review. Am J Chinese Med 2014;42:275-88.
9. Dong X, Zeng Y, Liu Y, You L, Yin X, Fu J, et al. Aloe-emodin: A review of its pharmacology, toxicity, and pharmacokinetics. Phytother Res 2020;34:270-81.
10. Lian LH, Park EJ, Piao HS, Zhao YZ, Sohn DH. Aloe emodin-induced apoptosis in t-HSC/Cl-6 cells involves a mitochondria-mediated pathway. Basic Clin Pharmacol 2005;96:495-502.
11. Friedman SL. Seminars in medicine of the Beth Israel Hospital, Boston. The cellular basis of hepatic fibrosis. Mechanisms and treatment strategies. New Engl J Med 1993;328:1828-35.
12. Woo SW, Nan JX, Lee SH, Park EJ, Zhao YZ, Sohn DH. Aloe emodin suppresses myofibroblastic differentiation of rat hepatic stellate cells in primary culture. Pharmacol Toxicol 2002;90:193-8.
13. Meng XM, Nikolic-Paterson DJ, Lan HY. TGF-beta: the master regulator of fibrosis. Nat Rev Nephrol 2016;12:325-38.
14. Yang F, Li T, Zhang XQ, Gong Y, Su H, Fan J, et al. Screening of active components in Astragalus mongholicus Bunge and Panax notoginseng formula for anti-fibrosis in CKD: nobiletin inhibits Lgals1/PI3K/AKT signaling to improve renal fibrosis. Renal Failure 2024;46:2375033.
15. He W, Dai C, Li Y, Zeng G, Monga SP, Liu Y. Wnt/beta-catenin signaling promotes renal interstitial fibrosis. J Am Soc Nephrol 2009;20:765-76.
16. Liu Y. Renal fibrosis: new insights into the pathogenesis and therapeutics. Kidney Int 2006;69:213-7.
17. Jia J, Xu LH, Deng C, Zhong X, Xie KH, Han RY, et al. Hederagenin ameliorates renal fibrosis in chronic kidney disease through blocking ISG15 regulated JAK/STAT signaling. Int Immunopharmacol 2023;118:110122.
18. Wu S, Ge Y, Lin K, Liu Q, Zhou H, Hu Q, et al. Telomerase RNA TERC and the PI3K-AKT pathway form a positive feedback loop to regulate cell proliferation independent of telomerase activity. Nucleic Acids Res 2022;50:3764-76.
19. Zhang Z, Wu W, Fang X, Lu M, Wu H, Gao C, et al. Sox9 promotes renal tubular epithelial−mesenchymal transition and extracellular matrix aggregation via the PI3K/AKT signaling pathway. Mol Med Rep 2020;22:4017-30.
20. Liu B, Deng J, Jie X, Lu F, Liu X, Zhang D. Protective effects of the Bupi Yishen formula on renal fibrosis through PI3K/AKT signaling inhibition. J Ethnopharmacol 2022;293: 115242.
21. Sharma M, Chuang WW, Sun Z. Phosphatidylinositol 3-kinase/Akt stimulates androgen pathway through GSK3beta inhibition and nuclear beta-catenin accumulation. J Biol Chem 2002;277:30935-41.
22. Singh SP, Tao S, Fields TA, Webb S, Harris RC, Rao R. Glycogen synthase kinase-3 inhibition attenuates fibroblast activation and development of fibrosis following renal ischemia-reperfusion in mice. Dis Model Mech 2015;8:931-40.
23. Bader GD, Hogue CW. An automated method for finding molecular complexes in large protein interaction networks. BMC Bioinform 2003;4:2.
24. Liu Y, Yang X, Gan J, Chen S, Xiao ZX, Cao Y. CB-Dock2: improved protein-ligand blind docking by integrating cavity detection, docking and homologous template fitting. Nucleic Acids Res 2022;50:W159-64.
25. Dou F, Liu Y, Liu L, Wang J, Sun T, Mu F, et al. Aloe-emodin ameliorates renal fibrosis via inhibiting PI3K/Akt/mTOR signaling pathway in vivo and in vitro. Rejuv Res 2019;22:218-29.
26. El-Abhar H, Abd EFM, Wadie W, El-Tanbouly DM. Cilostazol disrupts TLR-4, Akt/GSK-3beta/CREB, and IL-6/JAK-2/STAT-3/SOCS-3 crosstalk in a rat model of Huntington's disease. PLoS One 2018;13:e0203837.
27. Liu S, Chen X, Zhang S, Wang X, Du X, Chen J, et al. miR−106b−5p targeting SIX1 inhibits TGF−beta1−induced pulmonary fibrosis and epithelial−mesenchymal transition in asthma through regulation of E2F1. Int J Mol Med 2021;47:04855.
28. Wang Y, Liu P, Ma G, Wu C, Zhu W, Sun P, et al. Mechanism of dioscin ameliorating renal fibrosis through NF−kappaB signaling pathway−mediated inflammatory response. Mol Med Rep 2023;27:93.
29. Feng X, Chen L, Guo W, Zhang Y, Lai X, Shao L, et al. Graphene oxide induces p62/SQSTM-dependent apoptosis through the impairment of autophagic flux and lysosomal dysfunction in PC12 cells. Acta Biomater 2018;81:278-92.
30. Xi R, Pan S, Chen X, Hui B, Zhang L, Fu S, et al. HPV16 E6-E7 induces cancer stem-like cells phenotypes in esophageal squamous cell carcinoma through the activation of PI3K/Akt signaling pathway in vitro and in vivo. Oncotarget 2016;7:57050-65.
31. Tan RZ, Li JC, Liu J, Lei XY, Zhong X, Wang C, et al. BAY61-3606 protects kidney from acute ischemia/reperfusion injury through inhibiting spleen tyrosine kinase and suppressing inflammatory macrophage response. Faseb J 2020;34: 15029-46.
32. Xiao J, Meng XM, Huang XR, Chung AC, Feng YL, Hui DS, et al. miR-29 inhibits bleomycin-induced pulmonary fibrosis in mice. Mol Ther 2012;20:1251-60.
33. Qu H, Liu L, Liu Z, Qin H, Liao Z, Xia P, et al. Blocking TBK1 alleviated radiation-induced pulmonary fibrosis and epithelial-mesenchymal transition through Akt-Erk inactivation. Exp Mol Med 2019;51:1-17.
34. Ma Y, Wang M, Li N, Wu R, Wang X. Bleomycin-induced nuclear factor-kappaB activation in human bronchial epithelial cells involves the phosphorylation of glycogen synthase kinase 3beta. Toxicol Lett 2009;187:194-200.
35. Hill NR, Fatoba ST, Oke JL, Hirst JA, O'Callaghan CA, Lasserson DS, et al. Global prevalence of chronic kidney disease - A systematic review and meta-analysis. PLoS One 2016;11:e0158765.
36. Mu L, Zhu L, Feng Y, Chen N, Wang F, He L, et al. Nephropathy 1st inhibits renal fibrosis by activating the PPARgamma signaling pathway. Front Pharmacol 2022;13:992421.
37. Walther CP, Winkelmayer WC, Richardson PA, Virani SS, Navaneethan SD. Renin-angiotensin system blocker discontinuation and adverse outcomes in chronic kidney disease. Nephrol Dial Transpl 2021;36:1893-9.
38. Ni YH, Deng HF, Zhou L, Huang CS, Wang NN, Yue LX, et al. Ginsenoside Rb1 ameliorated bavachin-induced renal fibrosis via suppressing Bip/eIF2alpha/CHOP signaling-mediated EMT. Front Pharmacol 2022;13:872474.
39. Xiao D, Zhang Y, Wang R, Fu Y, Zhou T, Diao H, et al. Emodin alleviates cardiac fibrosis by suppressing activation of cardiac fibroblasts via upregulating metastasis associated protein 3.

Acta Pharm Sin B 2019;9:724-33.
40. Zhang Y, Song Z, Huang S, Zhu L, Liu T, Shu H, et al. Aloe emodin relieves Ang II-induced endothelial junction dysfunction via promoting ubiquitination mediated NLRP3 inflammasome inactivation. J Leukocyte Biol 2020;108:1735-46.
41. Liang Y, Jing Z, Deng H, Li Z, Zhuang Z, Wang S, et al. Soluble epoxide hydrolase inhibition ameliorates proteinuria-induced epithelial-mesenchymal transition by regulating the PI3K-Akt-GSK-3beta signaling pathway. Biochem Bioph Res Co 2015;463:70-5.
42. Cheng Y, Zhang J, Guo W, Li F, Sun W, Chen J, et al. Up-regulation of Nrf2 is involved in FGF21-mediated fenofibrate protection against type 1 diabetic nephropathy. Free Radical Bio Med 2016;93:94-109.
43. Eddy AA. Molecular basis of renal fibrosis. Pediatr Nephrol 2000;15:290-301.
44. Cai FF, Bian YQ, Wu R, Sun Y, Chen XL, Yang MD, et al. Yinchenhao decoction suppresses rat liver fibrosis involved in an apoptosis regulation mechanism based on network pharmacology and transcriptomic analysis. Biomed Pharmacother 2019;114:108863.
45. Wei S, Wang Q, Zhou H, Qiu J, Li C, Shi C, et al. miR-455-3p alleviates hepatic stellate cell activation and liver fibrosis by suppressing HSF1 expression. Mol Ther-Nucl Acids 2019;16:758-69.
46. Zhou T, Luo M, Cai W, Zhou S, Feng D, Xu C, et al. Runt-related transcription factor 1 (RUNX1) promotes TGF-beta-induced renal tubular epithelial-to-mesenchymal transition (EMT) and renal fibrosis through the PI3K subunit p110delta. eBioMedicine 2018;31:217-25.
47. Peng M, Zheng Z, Chen S, Fang L, Feng R, Zhang L, et al. Sensitization of non-small cell lung cancer cells to gefitinib and reversal of epithelial-mesenchymal transition by aloe-emodin via PI3K/Akt/TWIS1 signal blockage. Front Oncol 2022;12:908031.
48. Ma JW, Hung CM, Lin YC, Ho CT, Kao JY, Way TD. Aloe-emodin inhibits HER-2 expression through the downregulation of Y-box binding protein-1 in HER-2-overexpressing human breast cancer cells. Oncotarget 2016;7:58915-30.
49. Zhu X, Li Q, Hu G, Wang J, Hu Q, Liu Z, et al. BMS−345541 inhibits airway inflammation and epithelial−mesenchymal transition in airway remodeling of asthmatic mice. Int J Mol Med 2018;42:1998-2008.
50. Wang J, Hu K, Cai X, Yang B, He Q, Wang J, et al. Targeting PI3K/AKT signaling for treatment of idiopathic pulmonary fibrosis. Acta Pharm Sin B 2022;12:18-32.
51. Qin W, Cao L, Massey IY. Role of PI3K/Akt signaling pathway in cardiac fibrosis. Mol Cell Biochem 2021;476:4045-59.
52. Liu B, Lin J, Bai L, Zhou Y, Lu R, Zhang P, et al. Paeoniflorin inhibits mesangial cell proliferation and inflammatory response in rats with mesangial proliferative glomerulonephritis through PI3K/AKT/GSK-3beta pathway. Front Pharmacol 2019;10:978.
53. Hong H, Chen F, Qiao Y, Yan Y, Zhang R, Zhu Z, et al. GSK-3beta activation index is a potential indicator for recurrent inflammation of chronic rhinosinusitis without nasal polyps. J Cell Mol Med 2017;21:3633-40.
54. Hung PH, Hsu YC, Chen TH, Ho C, Lin CL. The histone demethylase inhibitor GSK-J4 is a therapeutic target for the kidney fibrosis of diabetic kidney disease via DKK1 modulation. Int J Mol Sci 2022;23:9407.
55. Ren J, Wei H, Sun J, Feng X, Zhang Y, Yuan H, et al. GSK3beta-dependent lysosome biogenesis: An effective pathway to mitigate renal fibrosis with LM49. Front Pharmacol 2022;13:925489.
56. Zhao JH. Mesangial cells and renal fibrosis. Adv Exp Med Biol 2019;1165:165-94.
57. Pathomthongtaweechai N, Chutipongtanate S. AGE/RAGE signaling-mediated endoplasmic reticulum stress and future prospects in non-coding RNA therapeutics for diabetic nephropathy. Biomed Pharmacother 2020;131:110655.
58. Liao Y, Tan RZ, Li JC, Liu TT, Zhong X, Yan Y, et al. Isoliquiritigenin attenuates UUO-induced renal inflammation and fibrosis by inhibiting Mincle/Syk/NF-kappa B signaling pathway. Drug Des Devel Ther 2020;14:1455-68.

Received: 7 May 2024. Accepted: 30 June 2025.

European Journal of Histochemistry 2025; 69:4228
doi:10.4081/ejh.2025.4228